

## A Double Arene Hydroxylation Mediated by Dicopper(II)–Hydroperoxide Species

Giuseppe Battaini,<sup>†</sup> Enrico Monzani,<sup>†</sup> Angelo Perotti,<sup>†</sup> Cristina Para,<sup>†</sup>  
Luigi Casella,<sup>\*†</sup> Laura Santagostini,<sup>‡</sup> Michele Gullotti,<sup>‡</sup> Renée Dillinger,<sup>§</sup>  
Christian Näther,<sup>§</sup> and Felix Tuczek<sup>§</sup>

Contribution from the Dipartimento di Chimica Generale, Università di Pavia,  
Via Taramelli 12, 27100 Pavia, Italy, Dipartimento C.I.M.A., Università di Milano,  
Centro CNR, Via Venezian 21, 20133 Milano, Italy, and Institut für Anorganische Chemie,  
Universität Kiel, Otto-Hahn-Platz 6/7, 24098 Kiel, Germany

Received August 9, 2002; E-mail: luigi.casella@unipv.it

**Abstract:** The dicopper(II) complex  $[\text{Cu}_2(\text{L})]^{4+}$  ( $\text{L} = \alpha, \alpha'$ -bis{bis[2-(1'-methyl-2'-benzimidazolyl)ethyl]amino}-*m*-xylene) reacts with hydrogen peroxide to give the dicopper(II)–hydroquinone complex in which the xylylene ring of the ligand has undergone a double hydroxylation reaction at ring positions 2 and 5. The dihydroxylated ligand 2,6-bis{(bis[2-(3-methyl-1*H*-benzimidazol-2-yl)ethyl]amino)methyl}benzene-1,4-diol was isolated by decomposition of the product complex. The incorporation of two oxygen atoms from  $\text{H}_2\text{O}_2$  into the ligand was confirmed by isotope labeling studies using  $\text{H}_2^{18}\text{O}_2$ . The pathway of the unusual double hydroxylation was investigated by preparing the two isomeric phenolic derivatives of **L**, namely 3,5-bis{(bis[2-(1-methyl-1*H*-benzimidazol-2-yl)ethyl]amino)methyl}phenol (**6**) and 2,6-bis{(bis[2-(1-methyl-1*H*-benzimidazol-2-yl)ethyl]amino)methyl}phenol (**7**), carrying the hydroxyl group in one of the two positions where **L** is hydroxylated. The dicopper(II) complexes prepared with the new ligands **6** and **7** and containing bridging  $\mu$ -phenoxo moieties are inactive in the hydroxylation. Though, the dicopper(II) complex **3** derived from **6** and containing a protonated phenol is rapidly hydroxylated by  $\text{H}_2\text{O}_2$  and represents the first product formed in the hydroxylation of  $[\text{Cu}_2(\text{L})]^{4+}$ . Kinetic studies performed on the reactions of  $[\text{Cu}_2(\text{L})]^{4+}$  and **3** with  $\text{H}_2\text{O}_2$  show that the second hydroxylation is faster than the first one at room temperature ( $0.13 \pm 0.05 \text{ s}^{-1}$  vs  $5.0(\pm 0.1) \times 10^{-3} \text{ s}^{-1}$ ) and both are intramolecular processes. However, the two reactions exhibit different activation parameters ( $\Delta H^\ddagger = 39.1 \pm 0.9 \text{ kJ mol}^{-1}$  and  $\Delta S^\ddagger = -115.7 \pm 2.4 \text{ J K}^{-1} \text{ mol}^{-1}$  for the first hydroxylation;  $\Delta H^\ddagger = 77.8 \pm 1.6 \text{ kJ mol}^{-1}$  and  $\Delta S^\ddagger = -14.0 \pm 0.4 \text{ J K}^{-1} \text{ mol}^{-1}$  for the second hydroxylation). By studying the reaction between  $[\text{Cu}_2(\text{L})]^{4+}$  and  $\text{H}_2\text{O}_2$  at low temperature, we were able to characterize the intermediate  $\eta^1:\eta^1$ -hydroperoxidicopper(II) adduct active in the first hydroxylation step,  $[\text{Cu}_2(\text{L})(\text{OOH})]^{3+}$  [ $\lambda_{\text{max}} = 342$  ( $\epsilon 12\,000$ ), 444 ( $\epsilon 1200$ ), and 610 nm ( $\epsilon 800 \text{ M}^{-1}\text{cm}^{-1}$ ); broad EPR signal in frozen solution indicative of magnetically coupled Cu(II) centers].

### Introduction

Synthetic copper complexes performing various types of oxygen activation processes have become increasingly important in the past decade,<sup>1</sup> in relation with the enzymatic reactions catalyzed by copper enzymes,<sup>2</sup> particularly tyrosinase, and the potential applications in catalytic transformations of organic substrates.<sup>3</sup> In general, in the best characterized systems, the adduct formed by dioxygen with a couple of copper atoms, in the form of either a  $\mu$ - $\eta^2:\eta^2$ -peroxidicopper(II) or a bis( $\mu$ -oxo)-dicopper(III) complex, performs C–H bond cleavage of the

ligand<sup>4–7</sup> or an exogenous substrate<sup>8</sup> with insertion of an oxygen atom. In other dinuclear copper systems performing ligand hydroxylation reactions, the putative copper–dioxygen intermediate could not be characterized due to its low stability even at low temperature.<sup>9</sup>

The key step in the monophenolase activity of tyrosinase is the reaction of the  $\eta^2:\eta^2$ -peroxidicopper(II) complex with the phenolic substrate to produce an *o*-quinone. Different pathways

<sup>†</sup> Università di Pavia.

<sup>‡</sup> Università di Milano.

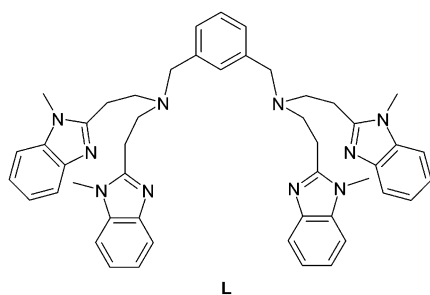
<sup>§</sup> Universität Kiel.

- (1) Karlin, K. D.; Zuberbühler, A. D. In *Bioinorganic Catalysis*, 2nd ed.; Reedijk, J., Bouwman, E., Eds.; Dekker: New York, 1999; pp 469–534.
- (2) (a) Solomon, E. I.; Sundaram, U. M.; Machonkin, T. E. *Chem. Rev.* **1996**, *96*, 2563–2605. (b) McGuirl, M. A.; Dooley, D. M. *Curr. Opin. Chem. Biol.* **1999**, *3*, 138–144. (c) Decker, H.; Dillinger, R.; Tuczek, F. *Angew. Chem., Int. Ed.* **2000**, *39*, 1591–1595. (d) Holland, P. L.; Tolman, W. B. *Coord. Chem. Rev.* **1999**, *190–192*, 855–869.
- (3) (a) Foote, C. S.; Valentine, J. S.; Greenberg, A.; Liebman, J. F., Eds. *Active Oxygen in Chemistry*; Chapman & Hall: London, 1995.

- (4) (a) Karlin, K. D.; Hayes, J. C.; Gultneh, Y.; Cruse, R. W.; McKown, J. W.; Hutchinson, J. P.; Zubieta, J. *J. Am. Chem. Soc.* **1984**, *106*, 2121–2128. (b) Karlin, K. D.; Nasir, M. S.; Cohen, B. I.; Cruse, R. W.; Kaderli, S.; Zuberbühler, A. D. *J. Am. Chem. Soc.* **1994**, *116*, 1324–1336. (c) Pidcock, E.; Obias, H. V.; Zhang, C. X.; Karlin, K. D.; Solomon, E. I. *J. Am. Chem. Soc.* **1998**, *120*, 7841–7847. (d) Becker, M.; Schindler, S.; Karlin, K. D.; Kaden, T. A.; Kaderli, S.; Palanché, T.; Zuberbühler, A. D. *Acc. Chem. Res.* **1997**, *30*, 139–147.
- (5) (a) Mahapatra, S.; Halfen, J. A.; Tolman, W. B. *J. Am. Chem. Soc.* **1996**, *118*, 11575–11586. (b) Mahapatra, S.; Kaderli, S.; Llobet, A.; Neuhold, Y.-M.; Palanché, T.; Halfen, J. A.; Young, V. G.; Kaden, T. A.; Que, L., Jr.; Zuberbühler, A. D.; Tolman, W. B. *Inorg. Chem.* **1997**, *36*, 6343–6356. (c) Holland, P. L.; Rodgers, K. R.; Tolman, W. B. *Angew. Chem., Int. Ed.* **1999**, *38*, 1139–1142. (d) Halfen, J. A.; Young, V. G.; Tolman, W. B. *Inorg. Chem.* **1998**, *37*, 2102–2103.

can be hypothesized for this reaction, and the currently accepted view suggests that either the side-on bound peroxy group directly attacks the substrate or a bis( $\mu$ -oxo) species resulting from cleavage of the O–O bond is the oxygenating species.<sup>2c,d</sup> A third pathway, involving a hydroperoxodicopper(II) species, is possible even though this implies previous protonation of the bound peroxide moiety. However, so far, hydroperoxodicopper(II) complexes have not been shown to be capable of supporting phenol hydroxylation reactions.

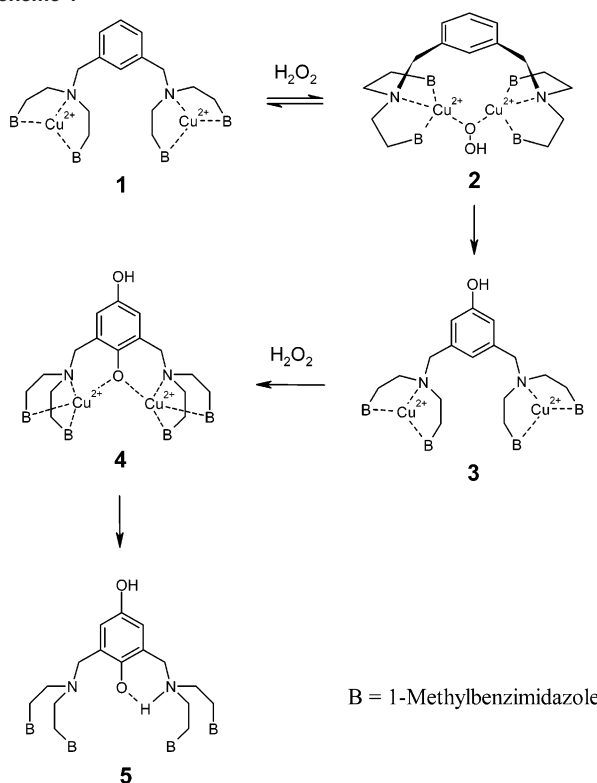
An interesting aspect of the aromatic ligand hydroxylation mediated by the peroxy complex derived from the reaction of  $[\text{Cu}_2(\text{XYL}-\text{H})]^{2+}$  with dioxygen, reported by Karlin et al. as the first example of tyrosinase model,<sup>4</sup> is that the reaction is not observed when the pyridine rings in the chelating arms of the *m*-xylyl-containing ligand are replaced by other nitrogen heterocycles such as imidazoles or benzimidazoles.<sup>9c,10</sup> For the dicopper(I) complex  $[\text{Cu}_2(\text{L})]^{2+}$ , **1**, where the ligand **L** contains *N*-methylbenzimidazole instead of pyridine rings,<sup>10b</sup> this feature has a positive effect from a practical point of view, since the dioxygen adduct of this complex is capable of hydroxylating an exogenous phenol, thereby exhibiting true tyrosinase-like activity.<sup>8</sup> However, the origin of this markedly different reactivity behavior between apparently strictly related peroxydicopper(II) systems is still unclear.



In Karlin's system, the xylyl ligand hydroxylation, to produce a  $\mu$ -hydroxo, $\mu$ -phenoxodicopper(II) species, can be achieved also by reacting the dinuclear Cu(II) complex,  $[\text{Cu}_2(\text{XYL}-\text{H})]^{4+}$ , and hydrogen peroxide.<sup>11</sup> In the latter case, although the intermediate active species could not be identified, a  $\eta^1:\eta^1$ -hydroperoxide complex has been proposed.<sup>11</sup> This performs the

- (6) (a) Itoh, S.; Nakao, H.; Berreau, L. M.; Kondo, T.; Komatsu, M.; Fukuzumi, S. *J. Am. Chem. Soc.* **1998**, *120*, 2890–2899. (b) Itoh, S.; Taki, M.; Nakao, H.; Holland, P. L.; Tolman, W. B.; Que, L., Jr.; Fukuzumi, S. *Angew. Chem., Int. Ed.* **2000**, *39*, 398–400. (c) Allen, W. E.; Sorrell, T. N. *Inorg. Chem.* **1997**, *36*, 1732–1734.
- (7) (a) Mahadevan, V.; Hou, Z.; Cole, A. P.; Root, D. E.; Lal, T. K.; Solomon, E. I.; Stack, T. D. P. *J. Am. Chem. Soc.* **1997**, *119*, 11996–11997. (b) Mahadevan, V.; DuBois, J. L.; Hedman, B.; Hodgson, K. O.; Stack, T. D. P. *J. Am. Chem. Soc.* **1999**, *121*, 5583–5584. (c) Mahadevan, V.; Henson, M. J.; Solomon, E. I.; Stack, T. D. P. *J. Am. Chem. Soc.* **2000**, *122*, 10249–10250.
- (8) Santagostini, L.; Gullotti, M.; Monzani, E.; Casella, L.; Dillinger, R.; Tuzcek, F. *Chem. Eur. J.* **2000**, *6*, 519–522.
- (9) (a) Casella, L.; Gullotti, M.; Pallanza, G.; Rigoni, L. *J. Am. Chem. Soc.* **1988**, *110*, 4221–4227. (b) Gelling, O. J.; van Bolhuis, F.; Meetsma, A.; Feringa, B. L. *J. Chem. Soc., Chem. Commun.* **1988**, 552–553. (c) Sorrell, T. N.; Vankai, V. A.; Garrity, M. L. *Inorg. Chem.* **1991**, *30*, 207–210. (d) Alzuet, G.; Casella, L.; Villa, M. L.; Carugo, O.; Gullotti, M. *J. Chem. Soc., Dalton Trans.* **1997**, 4789–4794. (e) Ghosh, D.; Mukherjee, R. *Inorg. Chem.* **1998**, *37*, 6597–6605. (f) Monzani, E.; Battaini, G.; Perotti, A.; Casella, L.; Gullotti, M.; Santagostini, L.; Nardin, G.; Randaccio, L.; Geremia, S.; Zanello, P.; Opromolla, G. *Inorg. Chem.* **1999**, *38*, 5359–5369.
- (10) (a) Sorrell, T. N.; Garrity, M. L. *Inorg. Chem.* **1991**, *30*, 210–215. (b) Casella, L.; Gullotti, M.; Radaelli, R.; Di Gennaro, P. *J. Chem. Soc., Chem. Commun.* **1991**, 1611–1612. (c) Casella, L.; Monzani, E.; Gullotti, M.; Cavagnino, D.; Cerina, G.; Santagostini, L.; Ugo, R. *Inorg. Chem.* **1996**, *35*, 7516–7525.

Scheme 1



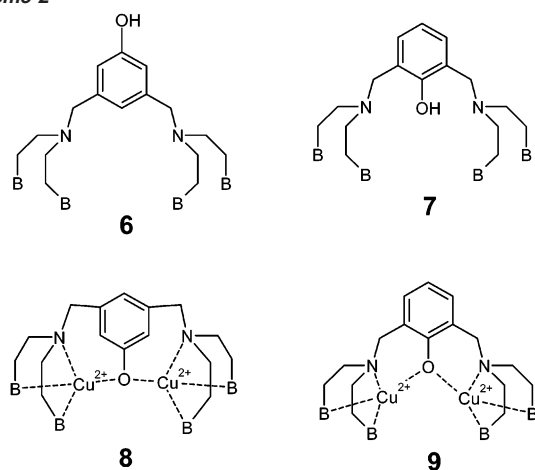
ligand hydroxylation according to an intermolecular mechanism which is different from the intramolecular pathway involved in the reaction between the corresponding dicopper(I) complex and dioxygen.<sup>4c</sup> In this paper, we report synthetic, mechanistic, and spectroscopic studies on a novel reaction between **1** and hydrogen peroxide, which produces a stable complex with the ligand containing a hydroquinone moiety, **4**, resulting from a double hydroxylation of the xylyl aromatic ring (Scheme 1, B = 1-methylbenzimidazole). This extremely facile reaction occurs in two successive steps. The first one is slower (at room temperature) and proceeds through a dicopper(II)–hydroperoxide complex, **2**, which evolves to the monohydroxylated complex **3**, where the aromatic position *meta* to the xylylene-diamino substituents has been hydroxylated. The second step is faster and involves binding of hydrogen peroxide to **3** and a second hydroxylation to give the hydroquinone complex **4**, from which the dihydroxylated ligand **5** can be isolated. This somewhat unexpected pathway was probed by preparing the two isomeric phenolic derivatives of the ligand **L**, namely **6** and **7** (Scheme 2), complex **3**, and the two  $\mu$ -phenoxodicopper(II) complexes derived from **6** and **7**, that is, **8** and **9**. The latter  $\mu$ -phenoxo complexes are inactive in the hydroxylation, whereas **3** reacts rapidly with  $\text{H}_2\text{O}_2$  to give **4**. The intermediate hydroperoxo complex  $[\text{Cu}_2(\text{L})(\text{OOH})]^{3+}$  was characterized at low temperature. This is the first dinuclear copper(II)–hydroperoxo complex in which the  $\text{HOO}^-$  moiety is the only bridging ligand between the copper(II) centers.

## Results and Discussion

**Aromatic Hydroxylation: Characterization of the Products.** The reaction between **1** and hydrogen peroxide produces

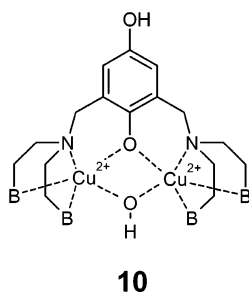
- (11) Cruse, R. W.; Kaderli, S.; Meyer, C. J.; Zuberbühler, A. D.; Karlin, K. D. *J. Am. Chem. Soc.* **1988**, *110*, 5020–5024.

Scheme 2

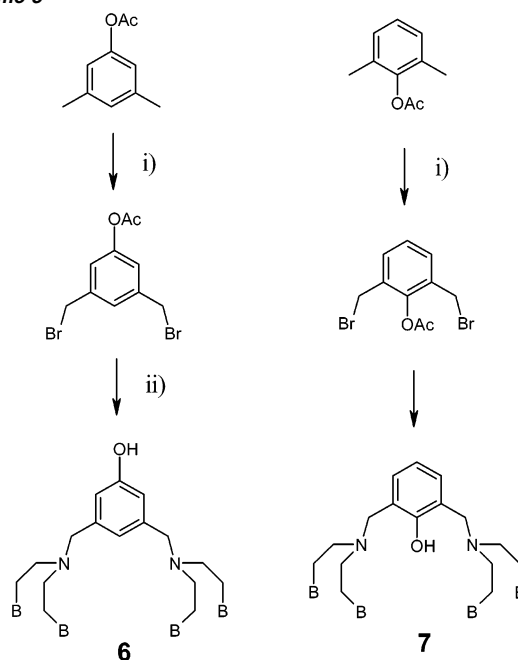


B = 1-Methylbenzimidazole

a species characterized by an intense absorption band near 345 nm ( $\epsilon \approx 9000 \text{ M}^{-1} \text{ cm}^{-1}$ ). The reaction occurs with a stoichiometry of 2  $\text{H}_2\text{O}_2$ :1  $[\text{Cu}_2(\text{L})]^{4+}$  (see Figure 1S in Supporting Information) and proceeds rapidly to completion when carried out on a preparative scale using a moderate excess of hydrogen peroxide. Chromatographic separation of the product mixture resulting from the reaction carried out in acetonitrile solution enabled us to isolate two products: a major green fraction consisting of the  $\mu$ -(4-hydroxy)-phenolate ( $\mu$ -hydroquinone) complex **4** and a minor, light brown fraction consisting of the  $\mu$ -hydroxo, $\mu$ -hydroquinone complex **10** (B = 1-methylbenzimidazole), which is probably formed spontaneously from **4** during workup.



The bis(hydroxylated) ligand **5** can be obtained from either **4** or **10** by removal of the copper ions using a base extraction procedure.<sup>4a</sup> After flash chromatographic purification, it is possible to isolate compound **5** in more than 80% yield. The  $^1\text{H}$  and  $^{13}\text{C}$  NMR characterization data of this compound confirm that the ligand **L** has undergone two oxygen atom insertions at positions 2 and 5 of the xylyl aromatic ring (see Figure 2S in Supporting Information and Experimental Section). The incorporation of two oxygen atoms from  $\text{H}_2\text{O}_2$  into the ligand was unequivocally confirmed by mass spectrometric analysis of **5**, which shows a cluster of peaks centered at  $m/z$  801.3. When the reaction between **1** and hydrogen peroxide was carried out using isotope labeled  $\text{H}_2^{18}\text{O}_2$  (90% enrichment), the dihydroxylated ligand isolated after decomposition exhibited an MS spectrum where the cluster of molecular peaks had shifted to  $m/z$  805.5 (ratio of  $\text{M}^+ / (\text{M}^+ + 2) / \text{M}^+ / (\text{M}^+ + 4) = 28:75:100$ , more than 80%  $^{18}\text{O}$  incorporated in each step) (see Figure 3S in Supporting Information). The free hydroquinoid ligand **5** is

Scheme 3<sup>a</sup>

<sup>a</sup> (i) *N*-bromosuccinimide; (ii) bis[2-(1-methyl-1*H*-benzimidazole-2-yl)ethyl]amine.

a somewhat unstable, photosensitive oily material which undergoes a slow oxidative degradation process in air at room temperature. The origin of the photosensitivity of **5** is quite certainly due to its moderate absorption near 340 nm ( $\epsilon \approx 3000 \text{ M}^{-1} \text{ cm}^{-1}$ ), which shifts to higher energy by the addition of acid and reveals that **5** assumes a zwitterionic structure. The same ligand hydroxylation of  $[\text{Cu}_2(\text{L})]^{4+}$  can be observed using *tert*-butyl hydroperoxide instead of  $\text{H}_2\text{O}_2$ , although in this case the reaction proceeds at a slower rate and, therefore, a much larger excess of oxidant must be used in order to observe significant conversion of **1** to **4**.

Since the hydroxylation occurs on the two carbon positions 2 and 5 of **L**, it could be anticipated that one of the phenoxodicopper(II) complexes **8** or **9** were intermediates of the reaction. The two putative intermediates were prepared for this purpose from the new phenolic ligands **6** and **7** (prepared according to Scheme 3). To our surprise, neither **8** nor **9** are able to support the ligand hydroxylation reaction by hydrogen peroxide observed with **1**. Complex **8** exhibits an extremely slow reaction with  $\text{H}_2\text{O}_2$ , but it is likely that this reaction is actually undergone by a small fraction of complex **3**, with unbound phenol, present in equilibrium in solution. In fact, compound **3** reacts rapidly with hydrogen peroxide to produce **4**. Attempts to prepare derivatives of complex **9** with either a protonated or *O*-acetylated phenol group were unsuccessful because in any conditions only the bridged  $\mu$ -phenoxo complex **9** spontaneously forms.

By following the reaction between **1** and  $\text{H}_2\text{O}_2$  in acetonitrile by IR spectroscopy, some significant changes can be observed in the 1100–1350  $\text{cm}^{-1}$ -range (Figure 1). In particular, a new band appears at 1304  $\text{cm}^{-1}$  concomitant with the transformation of **1** to **4**. Similar IR bands near 1300  $\text{cm}^{-1}$ , assigned to the phenolate  $\nu(\text{C}-\text{O})$  mode,<sup>12</sup> have been observed in the spectra

(12) Pyrz, J. W.; Karlin, K. D.; Sorrell, T. N.; Vogel, G. C.; Que, L., Jr. *Inorg. Chem.* **1984**, *23*, 4581–4584.

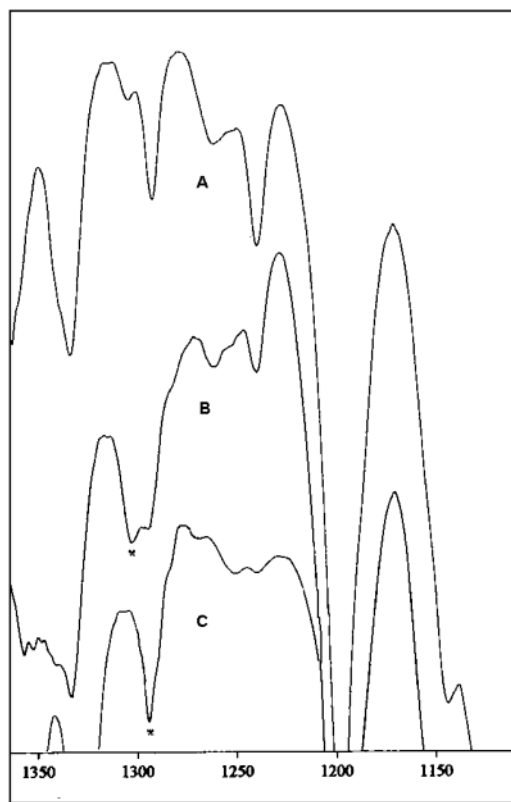


**Figure 1.** IR spectra recorded in acetonitrile solution of (A)  $[\text{Cu}_2(\text{L})][\text{ClO}_4]_4$  (20 mM); (B)  $[\text{Cu}_2(\text{L})][\text{ClO}_4]_4$  (20 mM) +  $\text{H}_2\text{O}_2$  (3-fold excess); and (C)  $[\text{Cu}_2(\text{L})][\text{ClO}_4]_4$  (20 mM) +  $\text{H}_2^{18}\text{O}_2$  (3-fold excess). Spectra B and C were recorded after a 2-h reaction time.

**Table 1.** UV–visible Spectral Data for Copper(II) Complexes in Acetonitrile Solution

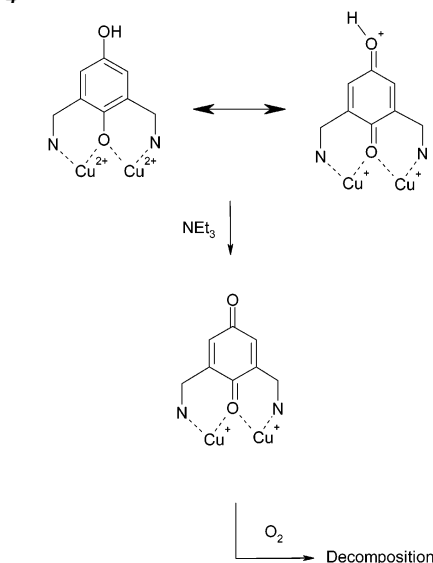
complex	IL $\lambda_{\text{max}}$ , nm ( $\epsilon$ , $\text{M}^{-1} \text{cm}^{-1}$ )	LMCT $\lambda_{\text{max}}$ , nm ( $\epsilon$ , $\text{M}^{-1} \text{cm}^{-1}$ )	d–d $\lambda_{\text{max}}$ , nm ( $\epsilon$ , $\text{M}^{-1} \text{cm}^{-1}$ )
<b>1</b>	273 (32 200)	310 sh (4000)	675 (450)
	280 (30 800)	410 sh (600)	850 (500)
<b>3</b>	270 (30 600)	318 sh (4600)	660 (300)
	278 (29 800)	360 sh (2000)	
<b>4</b>	273 (32 000)	345 (8500)	700 (250)
	280 (30 400)	420 sh (1400)	
<b>8</b>	272 (27 300)	314 (7200)	698 (700)
	280 (27 000)	410 sh (3200)	
<b>9</b>	272 (27 600)	344 (4000)	668 (250)
	280 (25 300)	424 (2300)	
<b>10</b>	273 (30 500)	320 sh (9600)	670 (220)
	280 (29 100)	345 (9200)	
		420 sh (1500)	

of related  $\mu$ -phenoxodicopper(II) complexes and are present also in the spectra of compounds **8** and **9**. In fact, the  $1304\text{-cm}^{-1}$  band undergoes a shift to  $1294\text{-cm}^{-1}$  when  $\text{H}_2^{18}\text{O}_2$  is used in the reaction with **1**, with a shift comparable to that reported for the formation of  $[\text{Cu}_2(\text{XYL}-\text{O})(\text{OH})]^{2+}$ .<sup>12,13</sup>

Both the bis(hydroxylated) complexes **4** and **10** exhibit a prominent absorption band at 345 nm ( $\epsilon \approx 9000\text{ M}^{-1} \text{cm}^{-1}$ ) and a weaker, broad absorption band centered near 420 nm ( $\epsilon \approx 1000\text{ M}^{-1} \text{cm}^{-1}$ ) (Table 1). The spectrum of **10** contains an additional, ill-defined absorption in the 300–330-nm range, likely due to hydroxo–Cu(II) ligand-to-metal charge-transfer transition (LMCT),<sup>14</sup> which overlaps with the strong intraben-

(13) Ling, J.; Farooq, A.; Karlin, K. D.; Loehr, T. M.; Sanders-Loehr, J. *Inorg. Chem.* **1992**, *31*, 2552–2556.

**Scheme 4**



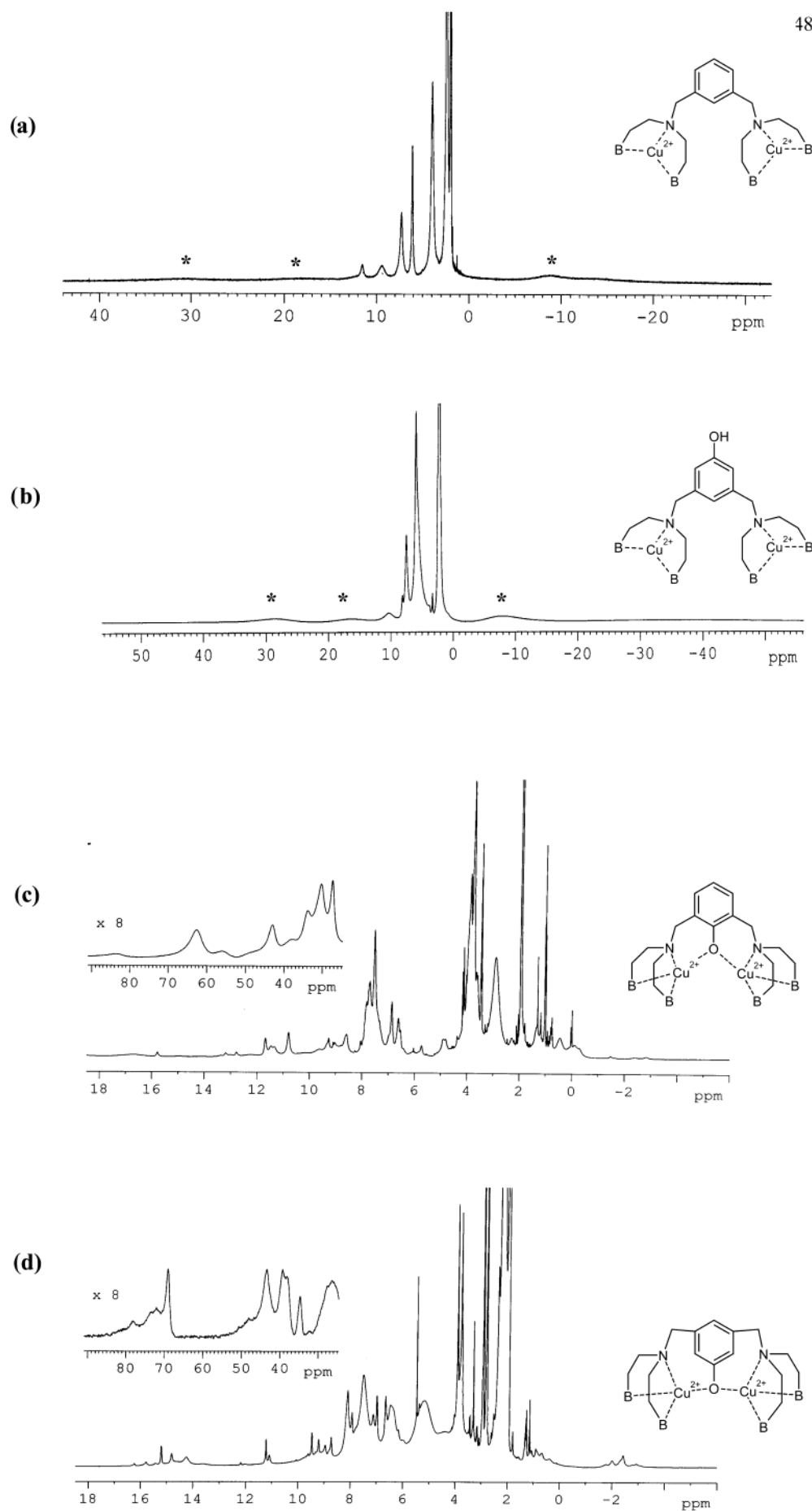
zimidazole bands at higher energy and the 345-nm band at lower energy. The origin of this 345-nm band is mostly due to a  $\pi \rightarrow \pi^*$  transition of the hydroquinone chromophore, since a similar absorption is present in the ligand, albeit with lower intensity. However, also weaker  $\pi(\text{benzimidazole}) \rightarrow \text{Cu(II)}$  LMCT transitions occur in the range between 300 and 400 nm, as is shown by the electronic spectrum of the starting  $[\text{Cu}_2(\text{L})]^{4+}$  complex.<sup>14</sup> It is likely that hydroquinone-to-copper LMCT bands contribute to both the intense 345-nm band and the weaker absorption band near 420 nm. The latter band is usually observed in the range between 400 and 470 nm, with variable intensity, for  $\mu$ -phenoxodicopper(II) complexes,<sup>13,15</sup> and occurs also in the spectra of **8** and **9**, but not in that of **3**, the near-UV spectrum of which resembles that of **1** (Table 1). Both the  $\mu$ -hydroquinone and  $\mu$ -phenoxo complexes exhibit d–d bands in the 650–700-nm range, indicative of an essentially square-pyramidal geometry for the Cu(II) centers.<sup>16</sup> It is worth noting that the Cu(II) coordination geometry in the starting complex **1** is essentially trigonal bipyramidal, but on conversion to the bis( $\mu$ -hydroxo) derivative  $[\text{Cu}_2(\text{L})(\text{OH})_2]^{2+}$ , the Cu(II) coordination sphere also changes to square pyramidal.<sup>14</sup> Upon addition of an excess base like triethylamine to solutions of **4** and **10**, the characteristic band at 344 nm quickly disappears and the solutions turn dark brown. As represented in Scheme 4, deprotonation of the hydroxyl group in **4** destabilizes the hydroquinone–Cu(II) moiety, giving rise to a fast oxidative decomposition.

The NMR spectra enable further characterization of the dicopper(II) complexes. As shown in Figure 2, the spectra of **1** and **3** are similar and contain broad, paramagnetically shifted signals in both the low field (between 15 and 30 ppm) and high field (between  $-5$  and  $-30$  ppm) regions. Other signals may be too broad to be detectable. The spectra of the  $\mu$ -phenoxo

(14) Casella, L.; Carugo, O.; Gullotti, M.; Garofani, S.; Zanello, P. *Inorg. Chem.* **1993**, *32*, 2056–2067.

(15) (a) Sorrell, T. N. *Tetrahedron* **1989**, *45*, 3–68. (b) Berends, H. P.; Stephan, D. W. *Inorg. Chem.* **1987**, *26*, 749–754. (c) Holz, R. C.; Brink, J. M.; Godena, F. T.; O'Connor, C. J. *Inorg. Chem.* **1994**, *33*, 6086–6092. (d) Holz, R. C.; Bradshaw, J. M.; Bennett, B. *Inorg. Chem.* **1998**, *37*, 1219–1225. (e) Torelli, S.; Belle, C.; Gautier-Luneau, I.; Pierre, J. L.; Saint-Aman, E.; Latour, J. M.; Le Pape, L.; Luneau, D. *Inorg. Chem.* **2000**, *39*, 3526–3536.

(16) Hathaway, B. J. In *Comprehensive Coordination Chemistry*; Wilkinson, G., Ed.; Pergamon Press: New York, 1987; Vol. 5, pp 533–774.



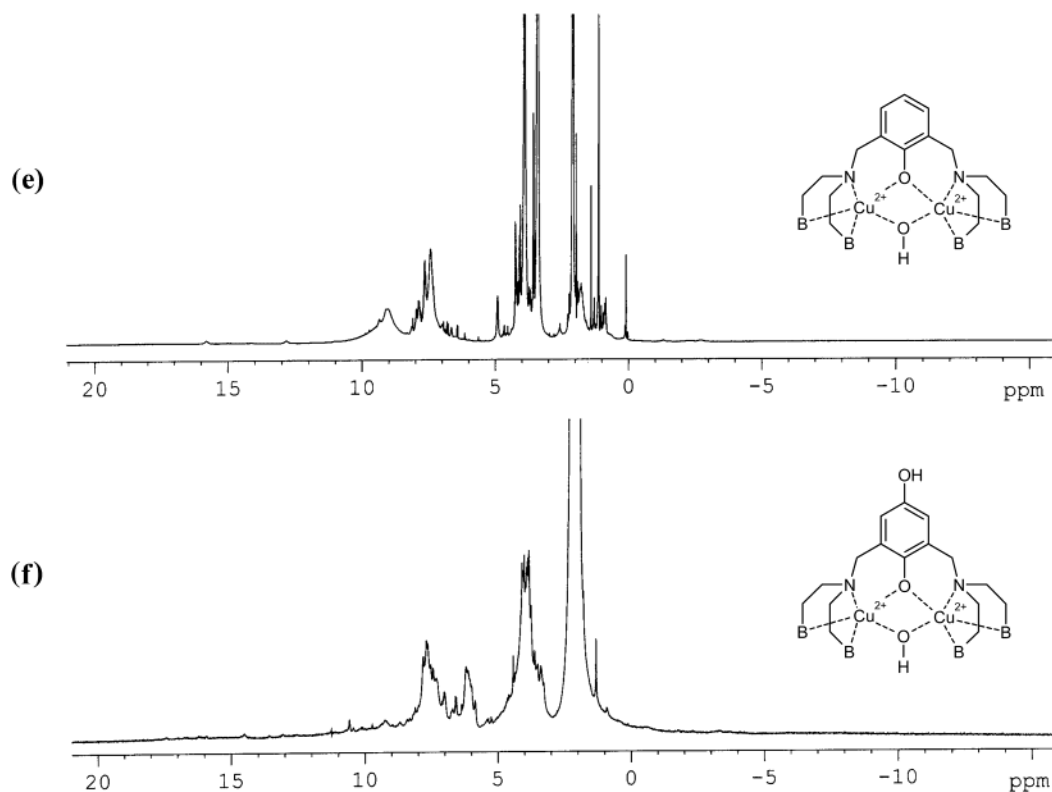
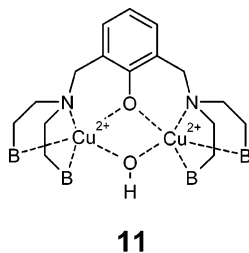


**Figure 2.** Proton NMR spectra of 1 mM  $\text{CD}_3\text{CN}$  solutions of (a) complex **1**; (b) complex **3**; (c) complex **9**; (d) complex **8**; (e) complex **11**; and (f) complex **10**.

complexes **8** and **9** contain several relatively sharp resonances at very low field (down to about 80 ppm), while those of the dibridged complexes **10** and **11** contain much sharper signals in the diamagnetic region (Figure 2), indicative of a strong coupling between the metal centers. While a detailed analysis



of these spectra and, more generally, the magnetic properties of the complexes are beyond the scope of the present investigation, it is clear that the NMR behavior confirms the presence or absence of single ( $\mu$ -phenoxo) or double ( $\mu$ -hydroxo, $\mu$ -phenoxo) bridges between the Cu(II) centers of the present dinuclear complexes.

**Crystal Structure of Complex 11.** Single crystals of compound **11** $[\text{ClO}_4]_2 \cdot \text{CH}_3\text{CN} \cdot (\text{C}_2\text{H}_5)_2\text{O}$  were obtained in the attempt to prepare the dicopper(II) complex of the *O*-acetylated ligand **7**. However, structure determination of the crystals isolated shows that the acetyl ligand was hydrolyzed on complex formation and a second hydroxo bridge formed during crystallization. The compound crystallizes in the triclinic centrosymmetric space group  $P\bar{1}$  with two formula units in the unit cell and all atoms located in general positions. Each copper(II) center is five-coordinated by the phenolate oxygen atom, three nitrogen atoms of the ligand, and the oxygen atom of the hydroxyl group

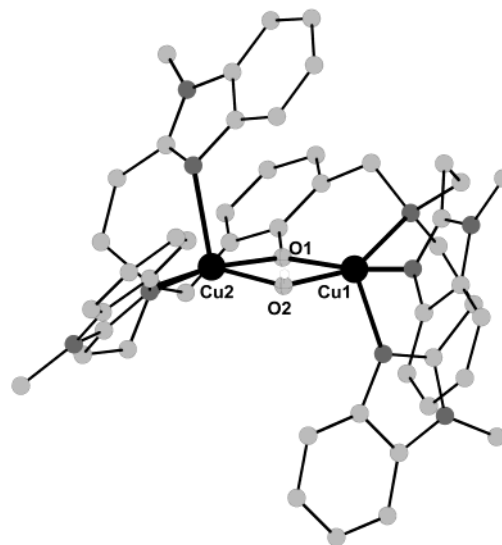
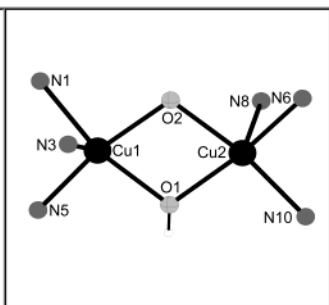


**Figure 3.** Molecular structure of the unit of complex **11** in the crystal structure of **11** $[\text{ClO}_4]_2 \cdot \text{CH}_3\text{CN} \cdot (\text{C}_2\text{H}_5)_2$ .

(Figure 3 and Table 2). The coordination polyhedron of the copper(II) centers can be described as distorted tetragonal pyramids sharing common edges each with one nitrogen atom on the top of the pyramid. The Cu–N distances to these nitrogen atoms are significantly longer compared to those in the basal plane of the pyramids (Table 2). Both copper(II) centers are connected via the phenolate oxygen atom of the ligand and one  $\mu$ -hydroxo bridge forming a nearly planar four-membered heteroring. The Cu–Cu distance amounts to 3.11(1) Å. The structure clearly shows that a bridging hydroperoxo group replacing the bridged hydroxo group would not be suitably

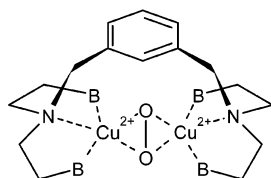
**Table 2.** Selected Bond Lengths (Å) and Angles (deg) for Complex **11**[Cu<sub>2</sub>(O<sub>2</sub>)<sub>2</sub>·CH<sub>3</sub>CN·(C<sub>2</sub>H<sub>5</sub>)<sub>2</sub>]

Cu(1)–O(1)	1.959 (2)		
Cu(1)–O(2)	1.986 (2)		
Cu(1)–N(1)	2.106 (2)		
Cu(1)–N(3)	2.175 (2)		
Cu(1)–N(5)	1.961 (2)		
Cu(2)–O(1)	1.982 (2)		
Cu(2)–O(2)	1.965 (2)		
Cu(2)–N(6)	2.066 (3)		
Cu(2)–N(8)	2.261 (2)		
Cu(2)–N(10)	1.991 (3)		
O(1)–Cu(1)–N(5)	164.6 (1)	O(1)–Cu(1)–O(2)	75.8 (1)
N(5)–Cu(1)–O(2)	92.7 (1)	O(1)–Cu(1)–N(1)	93.3 (1)
N(5)–Cu(1)–N(1)	93.0 (1)	O(2)–Cu(1)–N(1)	154.3 (1)
O(1)–Cu(1)–N(3)	94.6 (1)	N(5)–Cu(1)–N(3)	98.9 (1)
O(2)–Cu(1)–N(3)	110.0 (1)	N(1)–Cu(1)–N(3)	93.9 (1)
C(21)–N(1)–Cu(1)	113.8 (2)	C(29)–N(5)–Cu(1)	130.8 (2)
C(11)–N(1)–Cu(1)	113.6 (2)	C(7)–N(1)–Cu(1)	107.4 (2)
C(13)–N(3)–Cu(1)	122.7 (2)	C(19)–N(3)–Cu(1)	131.2 (2)
C(23)–N(5)–Cu(1)	121.5 (2)	C(2)–O(1)–Cu(1)	128.9 (2)
O(2)–Cu(2)–O(1)	75.7 (1)	O(2)–Cu(2)–N(10)	95.7 (1)
O(1)–Cu(2)–N(10)	168.5 (1)	O(2)–Cu(2)–N(6)	151.6 (1)
O(1)–Cu(2)–N(6)	92.1 (1)	N(10)–Cu(2)–N(6)	92.1 (2)



arranged for an intramolecular attack to the xylyl C–H bond *para* to the phenoxo group in the second hydroxylation step, but of course it may react intermolecularly with a second molecule of the complex.

**Low-Temperature Spectroscopy: Characterization of the Intermediates.** When a large excess of hydrogen peroxide (about 100-fold) is added to a solution of [Cu<sub>2</sub>(L)]<sup>4+</sup> in acetonitrile at –40 °C, a moderately intense band at 342 nm ( $\Delta\epsilon \approx 8600 \text{ M}^{-1}\text{cm}^{-1}$ ) and two weaker bands at 444 nm ( $\Delta\epsilon \approx 850 \text{ M}^{-1}\text{cm}^{-1}$ ) and 610 nm ( $\Delta\epsilon \approx 400 \text{ M}^{-1}\text{cm}^{-1}$ ) develop in the difference spectra (see Figure 4S in Supporting Information). The reaction is complete in 0.5 h, probably because hydrogen peroxide is partially frozen and undissolved in the solution. The UV bands do not decrease in intensity even upon applying several vacuum/argon cycles at low temperature. The spectral features and the irreversibility of the reaction exclude that this intermediate species can be the same  $\eta^2:\eta^2$ -peroxodicycopper(II) adduct that is formed by the reaction between [Cu<sub>2</sub>(L)]<sup>2+</sup> and O<sub>2</sub>, that is, [Cu<sub>2</sub>(L)(O<sub>2</sub>)]<sup>2+</sup> (**12**), which is characterized by  $\lambda_{\text{max}}$  at 362 ( $\epsilon \approx 15\,000$ ), 455 ( $\epsilon \approx 2000$ ), and 550 nm ( $\epsilon \approx 900 \text{ M}^{-1}\text{cm}^{-1}$ ).<sup>8</sup>



We thus propose that the bands that appear in the spectrum are associated with LMCT transitions of a dicopper(II)–hydroperoxide species with the  $\eta^1:\eta^1$  structure **2**. The bridging structure of this hydroperoxide complex is suggested by the pattern of LMCT bands, which is different for both the position

and number of components from those exhibited by mononuclear, terminally bound Cu–OOH complexes.<sup>17–21</sup>

Attempts to measure characteristic vibrations of this intermediate by resonance Raman spectroscopy using an excitation wavelength of 350 nm failed; that is, after addition of an excess of H<sub>2</sub>O<sub>2</sub> to a 10 mM solution of [Cu<sub>2</sub>(L)]<sup>4+</sup> in acetone/DMF or acetone/DMSO, no additional peaks could be detected. The subsequent addition of several equivalents of NEt<sub>3</sub> caused the solution to turn dark olive-green which is correlated with a shift of the CT band from 342 to 360 nm and the appearance of a shoulder at 420 nm. This optical spectrum is tentatively ascribed to the doubly bridged  $\mu$ -hydroxo  $\mu$ -hydroperoxo species. No Raman signals of this intermediate were detectable either, using excitation wavelengths of 350 or 413 nm. A possible reason for these findings might be the kinetic lability or, more likely, conformational flexibility of the hydroperoxo adducts, which is so important for the double hydroxylation, causes severe broadening of the Raman signals.

When the low-temperature solution of **2** is warmed to about –30 °C, the absorption bands of the hydroperoxo intermediate decrease quickly in intensity and are replaced by weaker spectral features (see Figure 4S in Supporting Information). A weaker and asymmetric band appears in the near-UV region, with a maximum near 370 nm in the difference spectrum ( $\Delta\epsilon \approx 2000 \text{ M}^{-1}\text{cm}^{-1}$ ). We identify this species as an hydroxo adduct of the monohydroxylated complex **3** on the basis of the near-UV feature in the difference spectrum, since hydroxo-to-Cu(II) LMCT transitions typically occur in the same range.<sup>9f,14</sup> When the low-temperature solution of this intermediate (with excess hydrogen peroxide present) is further warmed, some dramatic spectral changes occur. The band at 370 nm progressively decreases in intensity and around –20 °C is rapidly replaced by the stronger absorption band near 345 nm. The final spectrum corresponds to that previously described for complex **4**, containing the hydroquinone ligand **5**. Therefore, in the low-temperature experiment, we can clearly detect the intermediate and product of the first hydroxylation step. The second step involves the reaction between hydrogen peroxide and the intermediate hydroxo adduct of **3**, which is likely to give a second  $\mu$ -hydroperoxo adduct. But this intermediate is too reactive and cannot be detected. Also, compound **3** reacts rapidly with hydrogen peroxide in the same conditions to give the bis-(hydroxylated) compound **4**, as represented in Scheme 1, and even following the reaction at low temperature (down to –40 °C), no intermediate could be observed.

The hydroperoxo intermediate **2** was characterized also by EPR spectroscopy. As shown in Figure 4, the EPR spectrum of complex **1** in a solvent mixture of MeOH–DMF at –150 °C exhibits a well resolved signal for noninteracting Cu(II) centers. The EPR parameters,  $g_{\parallel} = 2.555$ ,  $A_{\parallel} = 172 \times 10^{-4} \text{ cm}^{-1}$ ,  $g_{\perp} = 2.05$ , with a partially resolved superhyperfine structure due to

- (17) (a) Wada, A.; Harata, M.; Hasegawa, K.; Jitsukawa, K.; Masuda, H.; Mukai, M.; Kitagawa, T.; Einaga, H. *Angew. Chem., Int. Ed.* **1998**, *37*, 798–799. (b) Chen, P.; Fujisawa, K.; Solomon, E. I. *J. Am. Chem. Soc.* **2000**, *122*, 10177–10193.
- (18) Solomon, E. I.; Tuzcek, F.; Root, D. E.; Brown, C. A. *Chem. Rev.* **1994**, *94*, 827–856.
- (19) Root, P. E.; Mahroof-Tahir, M.; Karlin, K. D.; Solomon, E. I. *Inorg. Chem.* **1998**, *37*, 4838–4849.
- (20) Karlin, K. D.; Ghosh, P.; Cruse, R. W.; Farooq, A.; Gultneh, Y.; Jacobson, R. R.; Blackburn, N. J.; Strange, R. W.; Zubieta, J. *J. Am. Chem. Soc.* **1988**, *110*, 6769–6780.
- (21) Mahroof-Tahir, M.; Murthy, N. N.; Karlin, K. D.; Blackburn, N. J.; Shaikm, S. N.; Zubieta, J. *Inorg. Chem.* **1992**, *31*, 3001–3003.

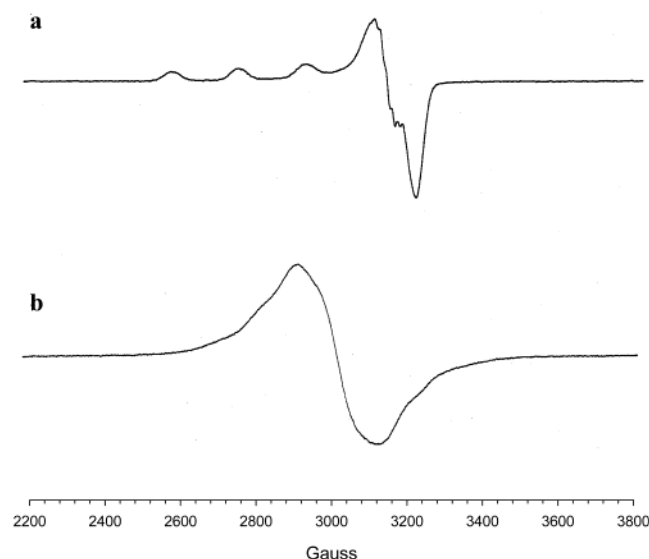


**Figure 4.** Frozen solution EPR spectra in MeOH–DMF (5:3, v/v), at  $-150$  °C, of complex **1** (a) and after adding excess  $\text{H}_2\text{O}_2$  at  $-80$  °C, in the presence of  $\text{NEt}_3$ , to obtain complex **2** (b).

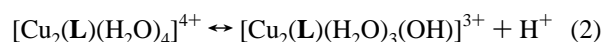
coupling with three nitrogen donors ( $A_{\text{N}}^{\text{II}} = 11.5$  G), are indicative of the presence of five-coordinated Cu(II) centers in a square-pyramidal geometry. Upon addition of excess  $\text{H}_2\text{O}_2$  at low temperature, the EPR spectrum of the resulting hydroperoxide adduct **2** changes to a fairly broad and unresolved signal at  $g \approx 2.12$ , consistent with a weakly antiferromagnetically coupled, dinuclear Cu(II) center containing a single bridging ligand.

**Ligand Protonation and Stability Constants of Copper(II)–L Complexes.** Since the reaction between  $[\text{Cu}_2(\text{L})]^{4+}$  and hydrogen peroxide occurs in a mixed aqueous–organic solvent, it is important to characterize the proton dissociation equilibria that metal-bound water molecules can undergo in the reaction conditions. Thus, the protonation and complex forming equilibria with  $\text{Cu}^{2+}$  of the ligand **L** were investigated potentiometrically in a mixture of acetonitrile–water, 4:1 (v/v). Five protonation

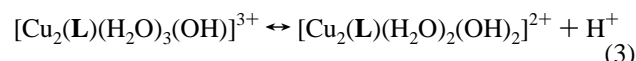
steps could be followed for **L**, and their cumulative  $\log \beta$  values were determined as follows: 8.04 (0.2), 14.94 (0.2), 19.86 (0.3), 23.98 (0.1), 25.85 (0.3). The ligand easily and simultaneously incorporates two copper(II) ions according to the equilibrium:



Successively, the complex containing two copper ions, each coordinated to three nitrogen atoms of the ligand and two water molecules,<sup>14</sup> undergoes a stepwise deprotonation of coordinated water molecules, as is shown in the species distribution diagram of Figure 5, according to the equilibria:



with a  $\text{p}K_{\text{a}1}$  of  $7.66 \pm 0.02$ , and



with a  $\text{p}K_{\text{a}2}$  of  $7.84 \pm 0.02$ . Both  $\text{p}K_{\text{a}}$  values are rather low and consistent with the formation of a bis( $\mu$ -hydroxo)dicopper(II) species. It can be noted that the first and the second deprotonation have similar  $\text{p}K_{\text{a}}$  values even though the charge decreases after the first step. This behavior is not surprising. As we previously noted,<sup>9f</sup> the monohydroxo species that forms after the first deprotonation step preorganizes the complex and makes easier the formation of the bridged complex containing the ring closed  $\text{Cu}_2(\text{OH})_2$  core.

**Kinetics.** Kinetic studies were performed to characterize both steps of the double hydroxylation reaction undergone by  $[\text{Cu}_2(\text{L})]^{4+}$  in the presence of hydrogen peroxide. When the reaction is studied by adding aqueous hydrogen peroxide to an acetonitrile solution of the complex, the development of the near-UV band near 350 nm due to **4** is preceded by a rapid decrease in intensity of the broad shoulder near 310 nm ( $k_{\text{obs}} = 3.3 \times 10^{-2} \text{ s}^{-1}$ ) (see Figure 1S in Supporting Information). This is due to an equilibration process of the species upon addition of the aqueous reagent, as it is shown by the fact that the process

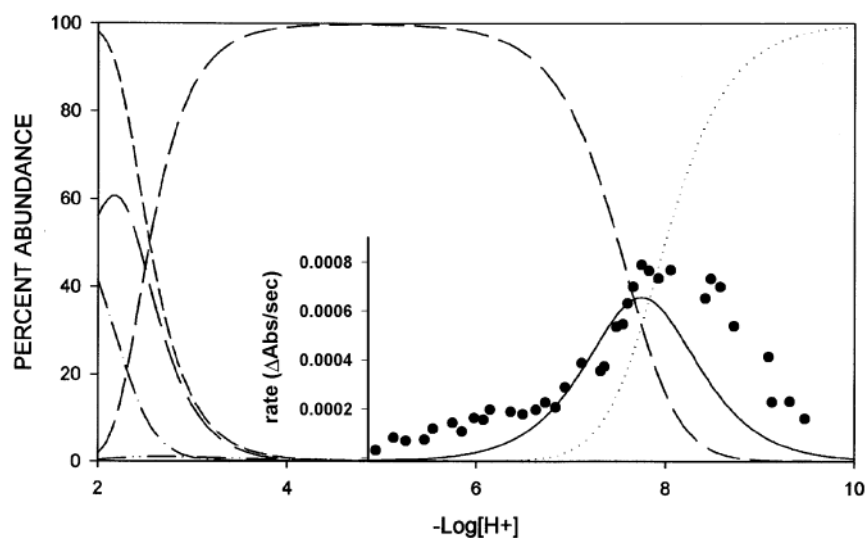


**Figure 5.** Species distribution in the 2 Cu/L system as a function of pH in acetonitrile/water solution (80:20, v/v): (---)  $[\text{Cu}_2(\text{L})(\text{OH})_2]^{2+}$ ; (—)  $[\text{Cu}_2(\text{L})(\text{OH})]^{3+}$ ; (····)  $[\text{Cu}_2(\text{L})(\text{OH})_2]^{2+}$ . The dot profile reproduced on the bottom right of the diagram shows the dependence of the rate of hydroxylation of complex  $[\text{Cu}_2(\text{L})]^{4+}$  (in  $\Delta\text{Abs}_{350}/\text{s}$  units) on the solution pH. The concentration of the complex was  $50 \mu\text{M}$ , while that of  $\text{H}_2\text{O}_2$  was  $0.2 \text{ mM}$  in all experiments. The reactions were studied in a 4:1 mixture of MeCN/aqueous 5 mM phosphate buffer at  $25 \pm 0.1$  °C; the pH of the solution was controlled by Gran's method. The species formed below pH 4 are protonated forms of **L** and free  $\text{Cu}^{2+}$  ion.

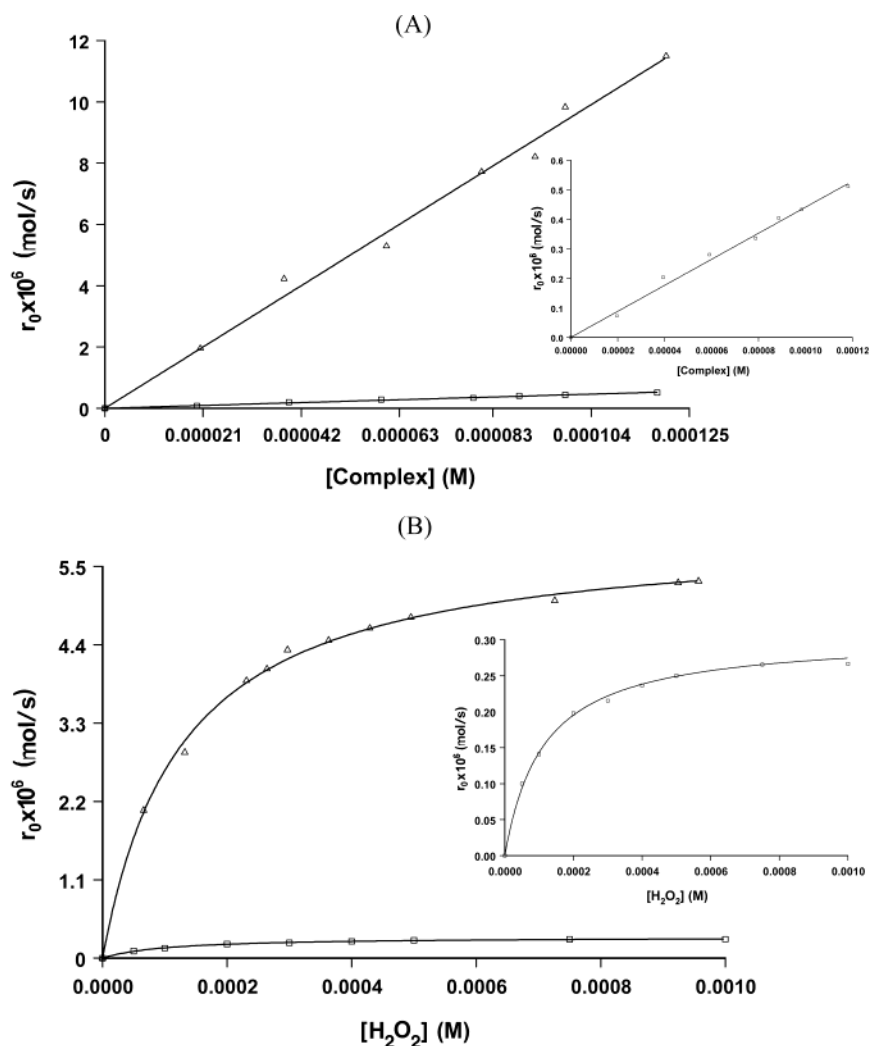


**Figure 6.** Dependence of the initial rates of hydroxylation of **1** ( $\square$ ) and **3** ( $\Delta$ ) by hydrogen peroxide as a function of the complex concentration (A) and hydrogen peroxide concentration (B). The insets show the plots referring to **1** on expanded scales.

can be reproduced by simply adding water to an acetonitrile solution of the complex. To avoid these problems, the kinetic experiments were performed in a solvent mixture of acetonitrile and aqueous phosphate buffer at pH 7.5, in a 4:1 ratio (v/v), at 25 °C. The first step was analyzed by studying the reaction of **1**, while the second step was studied employing complex **3**. Since the first hydroxylation reaction is slower than the second one, the intermediate compound **3** (Scheme 1) is not accumulated at room temperature. However, monitoring the development of the absorption band at 345 nm associated with compound **4** and considering the initial rate of the reaction ( $r_0$ ), we could analyze the mechanism of the rate-determining, first hydroxylation step. On the other hand, by studying the formation of **4** from **3** and hydrogen peroxide, we could obtain the rate of the second hydroxylation.

The rate dependence of the hydroxylation reactions was studied varying both the concentration of the complex and that of hydrogen peroxide. The dependence of the rate versus complex concentration was found to be linear for both **1** and **3** (Figure 6A), indicating that both hydroxylation reactions are intramolecular processes. This result accounts for the high percentage of the <sup>18</sup>O incorporation found in **5** when labeled hydrogen peroxide was used. The rate dependence of the hydroxylations of both **1** and **3** on hydrogen peroxide concentra-

tion exhibited a saturation behavior (Figure 6B). On the basis of these results, for both hydroxylation steps, the following simplified mechanism can be proposed:



where  $\text{L}' = \text{L}$  in the case of **1**, and  $\text{L}' = \mathbf{6}$  in the case of **3**. The kinetic parameters could be obtained by fitting the rate data to the equation corresponding to the previous preequilibrium scheme:

$$r_0 = \frac{k \cdot K \cdot [\text{Complex}] [\text{H}_2\text{O}_2]}{1 + K \cdot [\text{H}_2\text{O}_2]} \quad (6)$$

The following values of the kinetic parameters were obtained at 25 °C:

First hydroxylation:

$$k_1 = (5.0 \pm 0.1) \times 10^{-3} \text{ s}^{-1} \text{ and } K_1 = 9500 \pm 400 \text{ M}^{-1}$$

Second hydroxylation:

$$k_2 = (0.13 \pm 0.05) \text{ s}^{-1} \text{ and } K_2 = 7800 \pm 300 \text{ M}^{-1}$$

The slopes of the  $r_0$  versus [1] and  $r_0$  versus [3] plots are in perfect agreement with the extrapolated values of  $k$  and  $K$  for both steps. Thus, the second hydroxylation is about 25 times faster than the first one, which can be explained considering that the ligand **6** is considerably electron richer than **L**. The  $K_1$  and  $K_2$  constants can be considered as binding constants of hydrogen peroxide to **1** and **3**, respectively. The similarity between the two values indicates that the peroxide binds to species with the same ionic charge and, likely, also with the same binding mode in the two hydroxylation steps.

The rates of hydroxylation undergone by **1** and **3** display somewhat different temperature dependences, as shown by the Eyring plots included in the Supporting Information (Figure 5S). The activation parameters obtained for the two hydroxylation steps are the following:

First hydroxylation:

$$\Delta H^\ddagger = 39.1 \pm 0.9 \text{ kJ mol}^{-1}; \Delta S^\ddagger = -115.7 \pm 2.4 \text{ J K}^{-1} \text{ mol}^{-1}$$

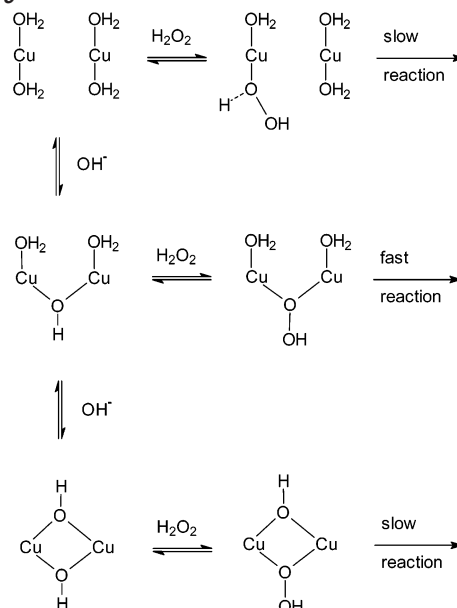
Second hydroxylation:

$$\Delta H^\ddagger = 77.8 \pm 1.6 \text{ kJ mol}^{-1}; \Delta S^\ddagger = -14.0 \pm 0.4 \text{ J K}^{-1} \text{ mol}^{-1}$$

The  $\Delta S^\ddagger$  values indicate that a more highly constrained transition state is required for the hydroxylation of **1** than for the hydroxylation of **3**. Though, in the more constrained excited state configuration, an easier and probably concerted bond-making and bond-breaking process accompanies the oxygen transfer reaction from the bound hydroperoxide to the ligand aromatic ring, as shown by the  $\Delta H^\ddagger$  data. The smaller activation entropy in the second hydroxylation is coupled to a larger activation enthalpy, and this results in a reduced difference in the rates of the two hydroxylations as the temperature is lowered. It is interesting to note that the activation parameters found for the ligand hydroxylation undergone by  $[\text{Cu}_2(\text{XYL}-\text{H})]^{2+}$  in the presence of  $\text{O}_2$  ( $\Delta H^\ddagger = 50 \text{ kJ mol}^{-1}$ ;  $\Delta S^\ddagger = -35 \text{ J K}^{-1} \text{ mol}^{-1}$ )<sup>1</sup> lie somewhat between those found here for the hydroxylations of **1** and **3** in the presence of  $\text{H}_2\text{O}_2$ , while smaller  $\Delta H^\ddagger$  and larger negative  $\Delta S^\ddagger$  values were found for the benzylic ligand hydroxylation undergone by the Cu(I) complex and  $\text{O}_2$  reported by Itoh et al.<sup>6a</sup> But, in the latter case, the association of two mononuclear units in a dimeric peroxo complex was involved.

For the first hydroxylation reaction, the pH dependence of the rate was also studied. The exact pH of the mixed solvent of acetonitrile–aqueous buffer was obtained by calibrating the electrodes according to Gran's method.<sup>22</sup> In these experiments, the reaction rates were studied using a hydrogen peroxide concentration that gives the highest rate of hydroxylation of **1** at pH 7.5 and 25 °C ( $2.5 \times 10^{-4} \text{ M}$ ). Interestingly, as reported in Figure 5, the rate dependence on pH follows an asymmetric bell shaped curve. The maximum rate is observed in the pH range around 8, corresponding to the conditions where the monohydroxo species  $[\text{Cu}_2(\text{L})(\text{OH})]^{3+}$  is maximized, according to the species distribution curve shown in the same figure. Taking into account the deprotonation of hydrogen peroxide, which is favored on increasing the pH, and that the  $[\text{Cu}_2(\text{L})(\text{OH})]^{3+}$  species is apparently much more reactive in the

Scheme 5

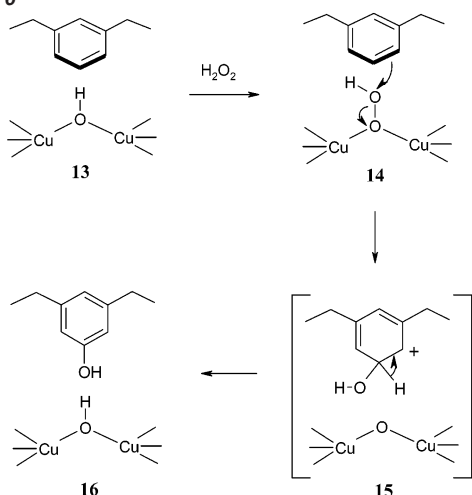


hydroxylation, we can explain the pH dependence of the rate according to the equilibria reported in Scheme 5, which shows that different hydroperoxo species can be formed in different conditions. In the acid pH range, binding of hydrogen peroxide to  $[\text{Cu}_2(\text{L})]^{4+}$  is unfavored because strong competition by protons prevents formation of the adduct with the hydroperoxide anion. Dicopper(II) hydroperoxo adducts can be formed in neutral and in basic conditions, but in the latter case, the simultaneous presence of a hydroxo bridge locks in the bound hydroperoxide, making impossible an intramolecular attack of this residue to the xylyl C–H bond of the ligand. It is only near neutral pH that the species containing a single hydroperoxo ligand exists in appreciable amount. This species has the conformational mobility and, possibly, also the electrophilicity to allow an intramolecular hydroxylation to occur. The pH dependence of the rate was not investigated for **3** because this compound readily gives rise to the unreactive  $\mu$ -phenoxo complex in a neutral medium. Neither doubly bridged  $\mu$ -hydroxo, $\mu$ -hydroperoxo nor  $\mu$ -phenoxo, $\mu$ -hydroperoxo complexes are able to support the aromatic hydroxylation.

**Mechanistic Considerations.** On the basis of the results described previously, it is possible to propose a mechanism for the double aromatic hydroxylation undergone by  $[\text{Cu}_2(\text{L})]^{4+}$  in the presence of hydrogen peroxide. In Scheme 6, the first hydroxylation step is illustrated, and it is assumed that the second hydroxylation step proceeds with a similar intramolecular mechanism. The monohydroxo derivative of the dinuclear complex **13** reacts with hydrogen peroxide to form the  $\eta^1:\eta^1$ -hydroperoxodicopper(II) complex **14**, which performs a regio-specific electrophilic attack on the aromatic nucleus of the ligand. The electrophilic nature of the reaction is shown by the fact that the second hydroxylation, occurring on the electron rich phenol nucleus of **3**, is faster than the first one on **1**. A key step is obviously the cleavage of the O–O bond of the hydroperoxo intermediate. A heterolytic cleavage, with a concerted attack on the aromatic nucleus, is preferred since this can better account for the regio-specificity of the reaction.

(22) Rossotti, F. J. C.; Rossotti, H. *J. Chem. Educ.* **1965**, *42*, 375–378.

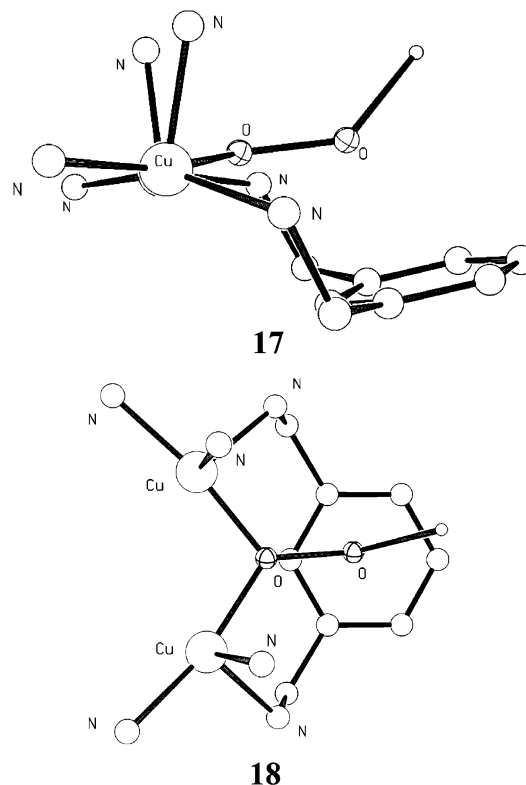
Scheme 6



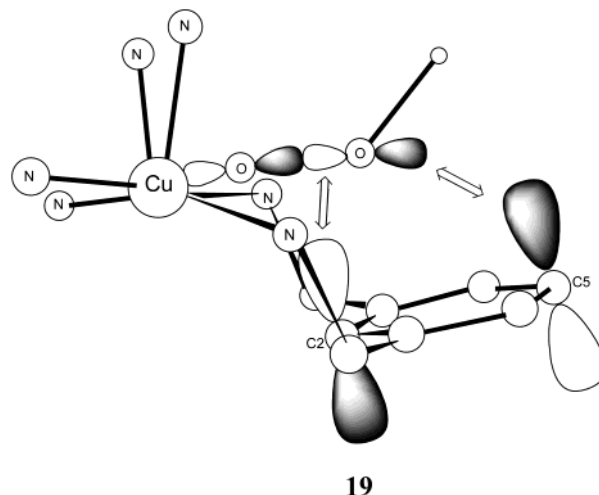
Homolysis of the hydroperoxide bond would produce a hydroxyl radical that could easily attack the aromatic nucleus in more than a single position, particularly in the second step, where the phenol nucleus of **3** has accessible ortho positions. Insertion of the OH group into the aromatic ring produces **15**, which, upon aromatization, yields the hydroxylated complex **16**.

Stereochemical aspects are extremely important in the present double hydroxylation reaction. Using a frontier molecular orbital description, Solomon hypothesized two possible pathways for the arene hydroxylation performed by the  $\eta^2:\eta^2$ -peroxodicopper(II) complex  $[\text{Cu}_2(\text{XYL}-\text{H})(\text{O}_2)]^{2+}$ .<sup>4c</sup> These depend on the configuration of the  $\text{N}_3\text{CuOOCuN}_3$  coordination units, containing approximately square-pyramidal copper centers, which involves either an eclipsed disposition of the two tridentate nitrogen donors and *cis* axial ligands, or a staggered disposition of the same donors and *trans* axial ligands. In the first case, the  $\text{Cu}_2\text{O}_2$  core is noncoplanar with the arene ring and the peroxide  $\sigma^*$  orbital can interact favorably with the HOMO of the arene. In the other case, the peroxide O–O atoms and the arene C2 and C5 atoms lie approximately on the same line but the plane of the arene ring is tilted with respect to the  $\text{Cu}_2\text{O}_2$  plane, as it is in  $[\text{Cu}_2(\text{XYL}-\text{O})(\text{OH})]^{2+}$ <sup>4a</sup> and in **11** (vide supra), and in these conditions, the peroxide  $\pi^*_\sigma$  component of the LUMO can overlap with the arene HOMO. The second pathway is favored for the arene hydroxylation undergone by  $[\text{Cu}_2(\text{XYL}-\text{H})(\text{O}_2)]^{2+}$ , which occurs at position 2 of the xylyl ring.<sup>4c</sup> In contrast, the hydroxylations proceed via hydroperoxo intermediates in the present case, and the first hydroxylation occurs at C5. As shown by the simple MM+ steric interaction minimization performed on **2** using the program Hyper Chem (Hyper Cube, release 5.01), when the two square-pyramidal copper(II) centers assume the eclipsed configuration, with *cis* axial ligands, the xylyl aromatic nucleus lies just below the OH group of the bound hydroperoxo moiety, as shown by structures **17** and **18**.

In this disposition, a direct overlap between the arene HOMO and the peroxide  $\sigma^*$  component is possible (**19**), and taking into account that the C2 and C5 atoms give larger orbital contributions to the HOMO,<sup>4c</sup> we can explain the regiochemistry of the two hydroxylations. The observation that, in the first step, hydroxylation at C5 is favored over hydroxylation at C2,



although, in **17** and **18**, C5 is farther away from the  $\beta$ -oxygen atom of the hydroperoxo group than C2, might be attributed to the fact that the  $p_\pi$ -orbital component of the arene HOMO at C5 has positive overlap with the  $p_\sigma$  orbital at the  $\beta$ -oxygen atom, whereas the  $p_\pi$ -orbital component of the arene HOMO at C2 is close to the nodal plane of the  $\sigma^*$  orbital, which reduces overlap. In addition, electron transfer from the arene HOMO into the hydroperoxo  $\sigma^*$  orbital acts to increase the O–O bond length and moves the  $\beta$ -oxygen atom toward C5, thus promoting a concerted O–O cleavage and aromatic hydroxylation at this position, in agreement with the activation data. Finally, both hydroxylations may require slight rotations of the arene ring around a C1–C3 axis in order to increase orbital overlap (counterclockwise for hydroxylation at C5 and clockwise for hydroxylation at C2; **19**).



In contrast to the  $\mu\text{-}\eta^1:\eta^1$ -hydroperoxodicopper(II) complex, the corresponding  $\mu\text{-}\eta^2:\eta^2$ -peroxodicopper(II) complex **12** was

found to be unable to support the hydroxylation of **L**.<sup>8</sup> This situation is thus different from that present in Karlin's [Cu<sub>2</sub>-(XYL-H)(O<sub>2</sub>)]<sup>2+</sup> complex,<sup>4c</sup> likely because of slight differences in the orientation of the pyridine rings in this complex with respect to the benzimidazole rings of **12**. These differences are determined by the bite angles of the heterocyclic donors and thus depend on the size of the heterocyclic rings, which differ in the two cases. As a result, both with eclipsed and staggered configurations of the chelating arms, the oxygen atoms of the side-on bound peroxide moiety are too far from the xylyl aromatic ring to promote an electrophilic attack, in contrast to Karlin's system.<sup>4c</sup> In addition, the orientation of the xylyl aromatic ring may be different in the two systems because it may be controlled by ring stacking interactions with the heterocyclic rings.

In conclusion, the present investigation describes a double arene hydroxylation mediated by hydroperoxodicopper(II) complexes bearing potential relevance for the mechanism of copper monooxygenases and, in particular, tyrosinase. Although the mechanisms proposed for tyrosinase generally involve a peroxo intermediate,<sup>2</sup> a rearrangement of the bound peroxide to hydroperoxide, with concomitant proton transfer, has been suggested by inhibition studies of the monophenolase reaction<sup>23</sup> and, more recently, by transient-phase kinetics of the diphenolase reaction.<sup>24</sup>

## Experimental Section

All reagents were purchased from commercial sources and used as received unless otherwise noted. DMF and acetonitrile were purified as described previously.<sup>9f</sup> The ligand **L-66** and the corresponding dinuclear complex [Cu<sub>2</sub>(**L**)](ClO<sub>4</sub>)<sub>4</sub> were prepared according to the published procedures.<sup>10b</sup> Bis[2-(1-methyl-1*H*-benzimidazol-2-yl)ethyl]amine was prepared as described previously.<sup>25</sup> Infrared spectra were recorded on a Perkin-Elmer Spectrum BX FT/IR instrument. Elemental analyses were obtained from the microanalytical laboratory of the Chemistry Department in Milano. NMR spectra were recorded on a Bruker Avance 400 spectrometer. EPR spectra were measured in frozen solutions using a Varian E-109 spectrometer operating at X-band frequencies. Optical spectra were measured on HP 8452A and 8453 diode array spectrophotometers. Electrospray ionization MS spectra were acquired using a Finnigan MAT system equipped with an ion trap detector. The solution was introduced into the electrospray source at 10 μL min<sup>-1</sup> using a syringe pump instrument. The ESI source was operated at 3.5 kV, the capillary temperature was set at 180 °C, and its voltage was at 10 V; the experiments were performed in positive ion mode.

**Acetic Acid 2,6-Dimethylphenyl Ester.** 2,6-Dimethylphenol (20 g, 164 mmol) was added to a mixture of acetic anhydride and pyridine 1:1 (v/v) (40 mL) in an ice bath. The pale yellow solution was stirred overnight at room temperature. The solvent was then removed by rotary evaporation. The remaining oil was washed with basic water and distilled under vacuum (bp 87 °C at 0.05 mmHg) (yield 75%). <sup>1</sup>H NMR (CDCl<sub>3</sub>): δ 7.1 (m, 3H, phenyl-H), 2.43 (s, 3H, CH<sub>3</sub>CO), 2.15 (s, 6H, CH<sub>3</sub>).

**Acetic Acid 2,6-Bis(bromomethyl)phenyl Ester.** Bromination of acetic acid 2,6-dimethylphenyl ester (20 g, 122 mmol) was carried out by refluxing it in CCl<sub>4</sub> (500 mL) with *N*-bromosuccinimide (43.5 g,

245 mmol) and traces of dibenzoyl peroxide. The refluxing flask was exposed to a 150-W tungsten lamp. After 1.5 h, the mixture was cooled to room temperature, filtered, and washed several times with basic water. The organic layer was dried using anhydrous MgSO<sub>4</sub>, and upon removal of the solvent, a light yellow oil was obtained. The crude product was dissolved in a mixture of CCl<sub>4</sub> (20 mL) and hexane (100 mL), and the solution was left for 1 day at 0 °C. Recrystallization of the white crystalline material that formed, in MeOH at -15 °C, yielded the purified product (yield 10%). <sup>1</sup>H NMR (CDCl<sub>3</sub>): δ 7.42 (d, 2H, phenyl-H), 7.25 (m, 2H, phenyl-H), 4.4 (s, 4H, CH<sub>2</sub>-Br), 2.48 (s, 3H, CH<sub>3</sub>CO).

**Acetic Acid 3,5-Dimethylphenyl Ester.** 3,5-Dimethylphenol (15 g, 0.123 mmol) was slowly added to a mixture of acetic anhydride and pyridine 1:1 (v/v) kept at 0 °C. Then, the resulting yellow solution was allowed to stir for 24 h at room temperature. Removal of the solvent followed by distillation under vacuum afforded the ester (yield 60%) (bp 72 °C at 0.1 mmHg). <sup>1</sup>H NMR (CDCl<sub>3</sub>): δ 6.92 (s, 1H, phenyl-H), 6.73 (s, 2H, phenyl-H), 2.38 (s, 6H, CH<sub>3</sub>), 2.32 (s, 3H, CH<sub>3</sub>CO).

**Acetic Acid 3,5-Bis(bromomethyl)phenyl Ester.** Bromination of acetic acid 3,5-dimethylphenyl ester (12 g, 73 mmol) was carried out by refluxing it in CCl<sub>4</sub> (500 mL) for 1.75 h with *N*-bromosuccinimide (26 g, 146 mmol) in the presence of a trace dibenzoyl peroxide. The refluxing mixture was also irradiated with a 150-W tungsten lamp. Then, the reaction mixture was cooled and washed with basic water, and the organic layer was dried over MgSO<sub>4</sub>. Upon rotary evaporation, the solvent was removed yielding an orange oil. This was dissolved in a mixture of CCl<sub>4</sub> (20 mL) and hexane (100 mL), and the solution was cooled for 1 day at 0 °C. The yellow crystalline solid that formed was recrystallized with hot methanol giving pure acetic acid 3,5-bis(bromomethyl)phenyl ester (yield 34%). <sup>1</sup>H NMR (CDCl<sub>3</sub>): δ 7.31 (s, 1H, phenyl-H), 7.13 (s, 2H, phenyl-H), 4.48 (s, 4H, CH<sub>2</sub>-Br), 2.33 (s, 3H, CH<sub>3</sub>CO).

**3,5-Bis({bis[2-(1-methyl-1*H*-benzimidazol-2-yl)ethyl]amino}-methyl)phenol (**6**).** This compound was obtained by reacting bis[2-(1-methyl-1*H*-benzimidazol-2-yl)ethyl]amine (330 mg, 1 mmol) with 3,5-bis(bromomethyl)phenyl ester (161 mg, 0.46 mmol) at reflux temperature in dry DMF (30 mL), under argon, and in the presence of anhydrous sodium carbonate (110 mg, 1 mmol), as a base, for 24 h. Then, a NaHCO<sub>3</sub>-saturated aqueous solution (10 mL) was added. The resulting brown mixture was stirred for 24 h. The solvent was removed by rotary evaporation, and the crude orange oil was chromatographed on silica gel, with MeOH/CH<sub>2</sub>Cl<sub>2</sub> 8:2 (v/v) as eluent, to afford **6** as a white powder (yield 26%). <sup>1</sup>H NMR (CD<sub>3</sub>OD): δ 7.53 (m, 4H, benzimidazole-H), 7.25 (m, 4H, benzimidazole-H), 7.18 (m, 8H, benzimidazole-H), 6.62 (s, 2H, phenyl-H), 6.41 (s, 1H, phenyl-H), 3.53 (s, 12H, N-CH<sub>3</sub>), 3.47 (s, 4H, CH<sub>2</sub>-phenyl), 2.85 (m, 16H, CH<sub>2</sub>). <sup>13</sup>C NMR (CD<sub>3</sub>OD): δ 157.5 (C), 154.5(C), 142.5 (C), 140.9 (C), 136.2 (C), 122.4 (CH), 122.2 (CH), 121.5 (CH), 117.8 (CH), 113.6 (CH), 109.8 (CH), 58.4 (CH<sub>2</sub>), 51.8 (CH<sub>2</sub>), 29.2 (CH<sub>3</sub>), 25.3 (CH<sub>2</sub>). UV-vis [MeOH, λ<sub>max</sub>, nm (ε, M<sup>-1</sup> cm<sup>-1</sup>): 252 (24 300), 276 (26 000), 282 (23 900), 310 (1450). IR (Nujol mull, cm<sup>-1</sup>): 3549 m, 3470 m, 3412 s, 1763 w, 1736 w, 1638 m, 1616 m, 1596 m, 1509 w, 1332 w, 1289 w, 1237 w, 1210 m, 1152 w, 1128 w, 1095 m, 1007 m, 969 w, 874 w, 847 w, 802 w, 766 w, 743 s, 722 m.

**2,6-Bis({bis[2-(1-methyl-1*H*-benzimidazol-2-yl)ethyl]amino}-methyl)phenol (**7**).** A mixture of acetic acid 2,6-bis(bromomethyl)phenyl ester (0.97 g, 2.8 mmol), bis[2-(1-methyl-1*H*-benzimidazol-2-yl)ethyl]amine (2 g, 6 mmol), anhydrous sodium carbonate (0.65 g, 6 mmol), and dry DMF (60 mL) was refluxed under argon for 51 h. The crude oily product obtained upon evaporation to dryness under vacuum of the mixture was found to be a mixture of **7** and acetic acid 2,6-bis-({bis[2-(1-methyl-1*H*-benzimidazol-2-yl)ethyl]amino}methyl)phenyl ester, as determined by TLC (MeOH/CH<sub>2</sub>Cl<sub>2</sub>, 8/2, v/v) and NMR. The crude mixture was stirred for 10 h at room temperature in a solution of MeOH (10 mL) and sodium bicarbonate-saturated water (10 mL). Then, upon reduction of the volume of the solution by rotary

(23) Conrad, J. S.; Dawso, S. R.; Hubbard, E. R.; Meyers, T. E.; Strothkamp, K. G. *Biochemistry* **1994**, *33*, 5739–5744.

(24) Rodríguez-Lopez, J. N.; Fenoll, L. G.; García-Ruiz, P. A.; Varon, R.; Tudela, J.; Thorneley, R. N. F.; García-Canovas, F. *Biochemistry* **2000**, *39*, 10497–10506.

(25) Casella, L.; Gullotti, M.; Redaelli, R.; Di Gennaro, P. *J. Chem. Soc., Chem. Commun.* **1991**, 1611–1612.

evaporation, a light yellow solid precipitated. This was purified by chromatography on silica gel, by eluting with a gradient of MeOH/CH<sub>2</sub>Cl<sub>2</sub>, which was varied from 1:1 to 8:2 (v/v), yielding pure **7** (yield 20%). <sup>1</sup>H NMR (CDCl<sub>3</sub>): δ 7.68 (m, 4H, benzimidazole-H), 7.20 (m, 12H, benzimidazole-H), 7.02 (d, 2H, phenyl-H), 6.68 (t, 1H, phenyl-H), 3.8 (s, 4H, CH<sub>2</sub>-phenyl), 3.45 (s, 12H, CH<sub>3</sub>-N), 3.15 (t, 8H, CH<sub>2</sub>), 3.01 (t, 8H, CH<sub>2</sub>). <sup>13</sup>C NMR (CDCl<sub>3</sub>): δ 156.1 (C), 153.8 (C), 143.0 (C), 136.0 (C), 129.5 (CH), 124.5 (C), 122.7 (CH), 122.53 (CH), 119.5 (CH), 118.9 (CH), 109.8 (CH), 56.0 (CH<sub>2</sub>), 51.5 (CH<sub>2</sub>), 30.2 (CH<sub>3</sub>), 26.3 (CH<sub>2</sub>). UV–vis [CH<sub>2</sub>Cl<sub>2</sub>, λ<sub>max</sub>, nm (ε, M<sup>-1</sup> cm<sup>-1</sup>): 256 (22 300), 278 (22 900), 284 (21 150), 336 (500). IR (Nujol mull, cm<sup>-1</sup>): 3286 s, 2726 w, 1732 w, 1614 m, 1594 m, 1505 m, 1331 w, 1261 m, 1233 w, 1150 w, 1123 m, 1095 m, 1090 m, 1007 m, 1006 m, 875 w, 842 w, 802 w, 766 m, 742 s.

**Copper Complexes 3[ClO<sub>4</sub>]<sub>4</sub> and 8[ClO<sub>4</sub>]<sub>3</sub>.** To a stirred solution of Cu(ClO<sub>4</sub>)<sub>2</sub>·6H<sub>2</sub>O (30 mg, 0.09 mmol) in methanol/aqueous 50 mM phosphate buffer pH 5.1, 30:1 (v/v) (15 mL), a solution of the ligand **6** (32 mg, 0.04 mmol) in MeOH (5 mL) was gently added. The solution was stirred for 30 min, and the light green precipitate that immediately formed was filtered, washed with a small portion of tetrahydrofuran, and dried under vacuum (yield 35%). This precipitate corresponds to **3[ClO<sub>4</sub>]<sub>4</sub>**. The light brown mother solution was allowed to stand in a refrigerator until a second precipitate formed. A light brown powder was collected by filtration and dried under vacuum (yield 40%). This product corresponds to **8[ClO<sub>4</sub>]<sub>3</sub>**.

**3[ClO<sub>4</sub>]<sub>4</sub>.** Anal. Calcd for C<sub>48</sub>H<sub>52</sub>N<sub>10</sub>O<sub>17</sub>Cl<sub>4</sub>Cu<sub>2</sub>: C, 44.01; H, 4.00; N, 10.69. Found: C, 44.02; H, 3.95; N, 10.31. IR (KBr, diffuse reflection, cm<sup>-1</sup>): 3420 br, 2936 s, 2023 m, 1658 s, 1617 m, 1496 m, 1485 w, 1458 s, 1414 m, 1390 w, 1332 w, 1301 w, 1260 m, 1100 br vs, 940 m, 871 m, 801 m, 760 m, 751 s, 627 s.

**8[ClO<sub>4</sub>]<sub>3</sub>.** Anal. Calcd for C<sub>48</sub>H<sub>51</sub>N<sub>10</sub>O<sub>13</sub>Cl<sub>3</sub>Cu<sub>2</sub>: C, 47.67; H, 4.25; N, 11.58. Found: C, 47.25; H, 4.15; N, 11.31. IR (KBr, diffuse reflection, cm<sup>-1</sup>): 3410 br, 2959 w, 2013 w, 1615 m, 1596 w, 1495 m, 1483 w, 1459 m, 1415 w, 1332 m, 1308 w, 1293 w, 1262 w, 1238 w, 1150 s, 1090 br vs, 940 w, 870 w, 854 w, 803 w, 793 w, 760 s, 751 s, 627 s.

**Complex 9[ClO<sub>4</sub>]<sub>3</sub>.** A sample of **7** (80 mg, 0.11 mmol) in CH<sub>2</sub>Cl<sub>2</sub> (2 mL) was slowly added to a solution of Cu(ClO<sub>4</sub>)<sub>2</sub>·6H<sub>2</sub>O (76 mg, 0.23 mmol) in dry acetonitrile (10 mL). The resulting green-yellow solution was stirred under argon for 30 min at room temperature. Diethyl ether was added until turbidity was observed. The solution was then cooled to 0 °C for 1 h, and the green solid that precipitated was filtered and dried under vacuum (yield 25%). Anal. Calcd for C<sub>48</sub>H<sub>51</sub>N<sub>10</sub>O<sub>13</sub>Cl<sub>3</sub>Cu<sub>2</sub>: C, 47.67; H, 4.25; N, 11.58. Found: C, 47.88; H, 4.64; N, 11.62. IR (KBr, diffuse reflection, cm<sup>-1</sup>): 3550 br, 3064 s, 2976 s, 2881 m, 2021 m, 1617 m, 1596 w, 1560 w, 1533 m, 1483 m, 1459 s, 1418 m, 1361 w, 1333 m, 1292 w, 1288 w, 1249 m, 1090 br vs, 1011 w, 982 w, 929 m, 866 w, 851 m, 760 s, 753 s, 625 s, 569 w.

**Isolation of the Hydroxylated Complexes 4[ClO<sub>4</sub>]<sub>3</sub> and 10[ClO<sub>4</sub>]<sub>2</sub>.** The complex [Cu<sub>2</sub>(L)]<sup>4+</sup> (100 mg, 0.07 mmol) was dissolved in acetonitrile (25 mL), and a concentrated aqueous solution of hydrogen peroxide (0.28 mmol) was added. The solution was allowed to react for 24 h under stirring at room temperature. Then, it was concentrated under reduced pressure and chromatographed on a Sephadex LH-20 column (1.5 × 40 cm<sup>2</sup>). Two bands were observed and collected separately: a major green fraction corresponding to complex **4** and a minor light brown fraction corresponding to **10**. The products were obtained upon rotary evaporation of the solutions resulting from chromatography.

**4[ClO<sub>4</sub>]<sub>3</sub>·MeCN.** Anal. Calcd for C<sub>50</sub>H<sub>54</sub>N<sub>11</sub>O<sub>14</sub>Cl<sub>3</sub>Cu<sub>2</sub>: C, 47.42; H, 4.30; N, 12.17. Found: C, 47.88; H, 4.63; N, 12.35. IR (KBr diffuse reflection, cm<sup>-1</sup>): 3400 br, 2050 w, 1619 m, 1501 m, 1485 m, 1461 m, 1454 m, 1418 m, 1304 w, 1291 w, 1240 w, 1100 s, 933 w, 859 w, 748 m, 625 m.

**10[ClO<sub>4</sub>]<sub>2</sub>.** Anal. Calcd for C<sub>48</sub>H<sub>52</sub>N<sub>10</sub>O<sub>11</sub>Cl<sub>2</sub>Cu<sub>2</sub>: C, 50.44; H, 4.59; N, 12.25. Found: C, 50.84; H, 4.85; N, 12.64. IR (KBr diffuse

reflection, cm<sup>-1</sup>) 3100 s, 2950 s, 1610 m, 1492 m, 1461 m, 1330 m, 1306 w, 1292 w, 1238 w, 1100 s, 1009 m, 929 w, 869 w, 750 m, 713 w, 622 m.

**Isolation of the Hydroxylated Ligand, 2,6-Bis([bis[2-(3-methyl-1H-benzimidazol-2-yl)ethyl]amino]methyl)benzene-1,4-diol (5).** The complex [Cu<sub>2</sub>(L)]<sup>4+</sup> (100 mg, 0.07 mmol) was dissolved in acetonitrile (25 mL), and concentrated aqueous hydrogen peroxide (0.28 mmol) was added. The solution was allowed to react for 24 h under stirring at room temperature. Then, it was concentrated under reduced pressure and chromatographed on a Sephadex LH-20 column (1.5 × 40 cm<sup>2</sup>). Both fractions which eluted were collected and combined; the solvent volume was reduced through rotary evaporation. The resulting concentrated solution was added to a chilled mixture of concentrated aqueous ammonia and CH<sub>2</sub>Cl<sub>2</sub> 1:1 (v/v, 100 mL) under stirring. The aqueous layer was separated and further extracted with cold CH<sub>2</sub>Cl<sub>2</sub> (50 mL, 3 times). The organic extracts were combined, washed with water, and then dried over MgSO<sub>4</sub>. Every step of the decomposition and extraction procedure was carried out at 5 °C using aluminum foil protection of the glassware from light exposure, to prevent any oxidative and photochemical decomposition of **5**. The final organic solution was purified by flash chromatography on a silica gel column, eluting with a solvent mixture of Et<sub>2</sub>O–iPrOH (5:4, v/v) to which an increasing amount of concentrated ammonia, from 1% to 15% (v/v), was added. The fractions containing the product were identified through the characteristic UV absorption of the benzimidazole residues (at 284, 276, and 254 nm) and collected. Upon evaporation of the solvent, a light yellow, somewhat air-sensitive oil was obtained (yield > 80%). <sup>1</sup>H NMR (CDCl<sub>3</sub>): δ 7.69 (m, 4H, benzimidazole-H), 7.25 (m, 14H, benzimidazole-H + phenyl-H), 3.72 (s, 4H, CH<sub>2</sub>-phenyl), 3.6 (s, 12H, CH<sub>3</sub>-N), 3.1 (t, 8H, CH<sub>2</sub>), 3.22 (t, 8H, CH<sub>2</sub>). <sup>13</sup>C NMR (CDCl<sub>3</sub>): δ 154.13 (C), 153.85 (C), 151.03 (C), 141.05 (C), 136.03 (C), 130.08 (CH), 122.71 (CH), 122.53 (CH), 119.36 (CH), 109.67 (CH), 58.81 (CH<sub>2</sub>), 53.82 (CH<sub>2</sub>), 30.20 (CH<sub>3</sub>), 26.37 (CH<sub>2</sub>). IR (liquid film, cm<sup>-1</sup>): 3340 s, 3059 w, 3007 w, 2937 m, 2852 w, 1666 m, 1629 m, 1510 s, 1469 s, 1442 s, 1402 m, 1330 m, 1282 m, 1238 m, 1217 m, 1151 w, 1126 w, 1095 w, 1028 w, 1008 w, 879 w, 753 s, 669 m. UV–vis [MeOH, λ<sub>max</sub>, nm (ε, M<sup>-1</sup> cm<sup>-1</sup>): 248 (31 400), 276 (26 600), 282 (25 500), 340 (3200). ESI–MS, *m/z*: 643.4 [MH–(CH<sub>2</sub>CH<sub>2</sub>Bz)]<sup>+</sup>, 801.3 [MH]<sup>+</sup>, 823.5 [M + Na]<sup>+</sup>.

The <sup>18</sup>O-labeled derivative of **5** was prepared by following the same procedure described previously but using smaller amounts of the reagents: [Cu<sub>2</sub>(L)]<sup>4+</sup> (0.004 mmol) and H<sub>2</sub><sup>18</sup>O<sub>2</sub> (90% <sup>18</sup>O, 2% in H<sub>2</sub>O, Icon Isotope, 0.016 mmol). ESI–MS, *m/z*: 647.5 [MH–(CH<sub>2</sub>CH<sub>2</sub>Bz)]<sup>+</sup>, 805.5 [MH]<sup>+</sup>, 827.3 [M + Na]<sup>+</sup>.

**Potentiometric Determinations.** Potentiometric titrations of **L** in the absence and in the presence of copper(II) ions were performed, with apparatus and methods described elsewhere,<sup>26</sup> in a mixture of acetonitrile–water 80:20 (v/v), made 0.1 M in ionic strength with NaClO<sub>4</sub> (50 mL) at 298 K. The electrodes were dipped for more than 1 h in the previously mentioned solvent mixture before standardization of the system, which was also made as previously described.<sup>26</sup> The HYPER-QUAD<sup>27</sup> program was used to process the data and calculate both the protonation and stability constants.

**Solution IR Measurements.** The hydroxylation reaction was investigated by IR spectroscopy in solution using a cell with a 0.05-cm path length and CaF<sub>2</sub> optical windows (HELLMA). The reaction solutions were prepared in a separate flask by adding 3 molar equiv. hydrogen peroxide (H<sub>2</sub>O<sub>2</sub>, 30% in water or H<sub>2</sub><sup>18</sup>O<sub>2</sub>, 90% <sup>18</sup>O, 2% in H<sub>2</sub>O, Icon Isotope) to an acetonitrile solution of [Cu<sub>2</sub>(L)]<sup>4+</sup> (20 mM, 200 μL). The solutions were allowed to react for 2 h, and then they were injected into the cell, and the spectra recorded. Blank spectra were recorded immediately after mixing of the reagents.

(26) Monzani, E.; Quinti, L.; Perotti, A.; Casella, L.; Gullotti, M.; Randaccio, L.; Geremia, S.; Nardin, G.; Faleschini, P.; Tabbi, G. *Inorg. Chem.* **1998**, *37*, 553–562.

(27) Sabatini, A.; Vacca, A.; Gans, P. *Coord. Chem. Rev.* **1982**, *120*, 389–405.

**Low-Temperature Spectroscopy.** The low-temperature spectra ( $-40\text{ }^{\circ}\text{C}$  and above) recorded during the reaction of  $[\text{Cu}_2(\mathbf{L})]^{4+}$  with hydrogen peroxide were obtained with a custom designed immersible fiber-optic quartz probe (HELLMA) fitted to a Schlenk vessel and connected with the HP 8452A diode array spectrophotometer. The experiment was performed using a solution of the complex in freshly distilled acetonitrile (0.15 mM) cooled in a chlorobenzene–acetone (8:2, v/v) liquid nitrogen cryogenic bath. To a chilled ( $-40\text{ }^{\circ}\text{C}$ ) solution of the complex (25 mL), 30% aqueous hydrogen peroxide was added ( $>100$ -fold molar excess), which quickly froze. Gradual warming of the mixture by swirling outside the bath was followed spectrophotometrically. When some changes became detectable in the spectra, the mixture was promptly chilled again to  $-40\text{ }^{\circ}\text{C}$ , and spectra of the reaction mixture were recorded during 1 h. Then, the solution was allowed to warm gently to  $-30\text{ }^{\circ}\text{C}$ , maintained at this temperature for about 1 h, and then slowly warmed again. Around  $-20\text{ }^{\circ}\text{C}$ , the spectral features started to change again, so warming was stopped and the temperature was maintained at about  $-20\text{ }^{\circ}\text{C}$  until the reaction appeared to be complete. Then, the solution was warmed gradually again to room temperature, but no further spectral changes were observed.

**Kinetics.** The kinetics of hydroxylation of **1** and **3** by hydrogen peroxide were studied in a magnetically stirred and thermostated optical cell with 1-cm path length, at  $25 \pm 0.1\text{ }^{\circ}\text{C}$ . The reactions were followed through the development of the near-UV band at 344 nm characteristic of the product. To reduce the effect of noise, the difference between the absorbance at 344 nm and that at 820 nm, where no absorption occurs, was monitored. The solvent employed for these measurements was a mixture of acetonitrile and aqueous 5 mM phosphate buffer pH 7.5 4:1 (v/v). The dependence of the initial rate of hydroxylation as a function of the complex concentration was studied maintaining the  $\text{H}_2\text{O}_2$  concentration 0.2 mM for **1** and 0.35 mM for **3**, while the concentration of the complexes was varied between 20  $\mu\text{M}$  and 120  $\mu\text{M}$ . The dependence of the initial rate of hydroxylation as a function of hydrogen peroxide concentration was investigated by adding a few microliters of concentrated  $\text{H}_2\text{O}_2$  (final concentration varied between 0.1 and 1 mM) to the solutions of the complexes, which were 50  $\mu\text{M}$  for **1** and 46  $\mu\text{M}$  for **3**. The experiments to determine the hydroxylation rate of **1** as a function of pH were carried out on solutions 50  $\mu\text{M}$  in the complex and 200  $\mu\text{M}$  in  $\text{H}_2\text{O}_2$ , by rapidly adding small quantities of NaOH or  $\text{HClO}_4$  to the appropriate pH value and immediately starting the optical readings. The exact pH of the solvent mixture was determined by calibration of the electrode through the addition of measured quantities of standard perchloric acid solution, according to Gran's method.<sup>22</sup> The pH interval covered by the kinetic experiments was between 5 and 10. The initial rates were determined from the absorbance versus time curves, typically in the initial 50–60-s reaction time.

The kinetics of the fast initial phase preceding the hydroxylation was studied using an Applied Photophysics stopped flow system (RS-100), with a dead time of 1 ms and a 1-cm path length, coupled with a HP 8452A diode array spectrophotometer. In these experiments, a  $\text{CH}_3\text{CN}$  solution of **1** (100  $\mu\text{M}$ ) was mixed with a 2 mM hydrogen peroxide solution obtained by diluting the concentrated aqueous solution with acetonitrile. The experiment was repeated in the same conditions using a 2 mM solution of water in acetonitrile. The cell and the reactant solutions were thermostated at  $25 \pm 0.1\text{ }^{\circ}\text{C}$ . Mixing of the solutions in the stopped flow cuvette reduces the reactant concentrations to one-half.

**Crystal Structure Determination of 11.** A sample of solid  $\text{Cu}(\text{ClO}_4)_2 \cdot 6\text{H}_2\text{O}$  (0.34 mmol) was added to a solution of *O*-acetylated **7**

(0.17 mmol) in acetonitrile (8 mL). The dark green solution was stirred for 1 h, and then small amounts of diethyl ether were added until turbidity was observed. The mixture was allowed to stand overnight in a refrigerator. The green precipitate was filtered off, and vapors of diethyl ether were diffused into the filtrate. The crystallized material consists of light green plates of  $11[\text{CLO}_4]_2 \cdot \text{CH}_3\text{CN} \cdot (\text{C}_2\text{H}_5)_2\text{O}$ . These green plates decompose within a few minutes, presumably due to the loss of solvent molecules incorporated in the crystals.

X-ray crystallographic studies were done using an imaging plate diffraction system (IPDS) from STOE & CIE (Mo  $K\alpha$  radiation). The lattice parameters were obtained from 7998 reflections in the range of  $24^\circ \leq 2\theta \leq 38^\circ$  ( $a = 13.994(2)\text{ \AA}$ ,  $b = 15.092(2)\text{ \AA}$ ,  $c = 15.314(2)\text{ \AA}$ ,  $\alpha = 77.75(1)^\circ$ ,  $\beta = 78.66(1)^\circ$ ,  $\gamma = 74.26(1)^\circ$ ,  $V = 3008.4(5)\text{ \AA}^3$  ( $T = 150\text{ K}$ ),  $Z = 2$ ,  $\rho_{\text{ber}} = 1.371\text{ g cm}^{-3}$ , triclinic, space group  $P\bar{1}$  (No. 2),  $\mu = 0.86\text{ mm}^{-1}$ , 23 088 measured reflections in the range of  $3^\circ \leq 2\theta \leq 55^\circ$ , 10 896 independent reflections used for refinement ( $R_{\text{int}} = 0.0621$ ), 8958 independent reflections with  $F_o > 4\sigma(F_o)$ ). Structure solution was performed with SHELXS-94, and structure refinement was done with full-matrix least squares against  $F^2$  using SHELXL-97 (726 refined parameters,  $w = 1/[\sigma^2(F_o^2) + (0.0863P)^2 + 1.07P]$ ,  $R_1$  for 8958 reflections with  $F_o > 4\sigma(F_o) = 0.0489$ ,  $wR2$  for all 10 896 reflections = 0.1436, GOOF = 1.048, residual electron density =  $0.64/-0.76\text{ e/\AA}^3$ . All non-hydrogen atoms except one carbon atom of the diethyl ether molecule which is disordered were refined with anisotropic displacement parameters. All hydrogen atoms were placed in ideal positions and refined with isotropic displacement parameters [ $U_{\text{iso}} = 1.2U_{\text{eq}}(\text{C}_{\text{aromatic/methylene}}) = 1.5U_{\text{eq}}(\text{C}_{\text{methyl/hydroxyl}})$ ] using the riding model with the parameters C–H (aromatic) 0.95  $\text{\AA}$ , C–H (methylene) 0.99  $\text{\AA}$ , C–H (methyl) 0.98  $\text{\AA}$ , and C–H (hydroxyl) 0.85  $\text{\AA}$ . The position of the hydrogen atom bound to O2 was located first from a difference map. Because refinement with varying coordinates and displacement parameters was not possible, this atom was also refined using a riding model. The crystal contains additional solvent molecules, presumably diethyl ether, in holes of the structure for which no successful structure model can be found. Therefore, the data were corrected for the disordered solvent using the “Squeeze” option in Platon. The analysis yields a total potential solvent accessible volume of 335  $\text{\AA}^3$ . The electron count per cell 54 was not included in the calculated density and in  $F(000)$ .

**Acknowledgment.** This work was supported by grants from FAR (University of Pavia) and the Italian CNR. Support by the European COST and INTAS programs is also acknowledged. L.S. was supported by a fellowship by CIRCMSB.

**Supporting Information Available:** Crystallographic data including experimental details of the structure determination and tables with bond lengths, bond angles, atomic coordinates as well as equivalent isotropic and anisotropic displacement parameters are provided in PDF format; also included are five figures presenting optical spectral changes observed in the hydroxylation of complex **1**, the aromatic region of the  $^{13}\text{C}$ – $^1\text{H}$  HMQC NMR spectrum of the dihydroxylated ligand **5**, the MS spectra of **5** and its  $^{18}\text{O}$  analogue, the low-temperature spectral changes associated with the formation and reaction of the hydroperoxidicopper(II) intermediate **2**, and the Eyring plots related to the hydroxylation of **1** and **3**. This material is available free of charge via the Internet at <http://pubs.acs.org>.

JA0280776